Fluid Phase Equilibria 596 (2025) 114432

Contents lists available at ScienceDirect

Fluid Phase Equilibria

journal homepage: www.sciencedirect.com/journal/fluid-phase-equilibria

Speed-of-sound measurements in liquid *n*-heptane and 2,2,4-trimethylpentane (isooctane)

T. Dietl, A. El Hawary, K. Meier *

Institut für Thermodynamik, Helmut-Schmidt-Universität/Universität der Bundeswehr Hamburg, Holstenhofweg 85, 22043, Hamburg, Germany

ARTICLE INFO

Keywords:
n-Heptane
High pressure
Isooctane
Pulse-echo method
Speed of sound

ABSTRACT

This paper reports comprehensive and accurate measurements of the speed of sound in liquid *n*-heptane and 2,2,4-trimethylpentane (isooctane). The measurements were carried out by a double-path-length pulse-echo technique and cover the temperature range between 200 K and 420 K with pressures up to 100 MPa. The expanded uncertainties (coverage factor $k = 2$) amount to 2.1 mK in temperature, 0.005% in pressure, 0.02% in speed of sound in *n*-heptane, and 0.015% in speed of sound in isooctane, with the exception of a few state points at low pressures, where it increases up to 0.03% for *n*-heptane and up to 0.035% for isooctane. Our data are more accurate than previously published data for both fluids. The measurements for isooctane extend the range in which the speed of sound had been measured before from 293 K down to 200 K and from 373 K up to 420 K. We also provide accurate correlations for the speed of sound as a function of temperature and pressure in the range of our measurements. Our data can contribute to developing new, more accurate equations of state for both fluids.

1. Introduction

In previous works, we measured comprehensive and accurate data sets for the speed of sound c in the liquid and partially also in the supercritical regions of the alkanes ethane [1], propane [2], *n*-butane [3], 2-methylpropane (isobutane) [4], *n*-pentane [5], and 2-methylbutane (isopentane) [5] in a wide range of temperature and at elevated pressures up to 100 MPa using a double-path-length pulse-echo technique. In this work, we continue these studies with measurements of the alkanes *n*-heptane and 2,2,4-trimethylpentane (isooctane) in the liquid region. *n*-Heptane and isooctane are used to define the octane rating scale of fuels [6]. *n*-Heptane forms the standard zero point and isooctane the standard 100 point of the scale. Points of the scale between zero and 100 are realized by binary mixtures of *n*-heptane and isooctane, where the volume fraction of isooctane defines the octane number of the mixture [7]. *n*-Heptane occurs as a minor component in gasoline and is often used as a nonpolar solvent in various industrial applications. For these applications and for the development of an accurate equation of state for binary mixtures of *n*-heptane and isooctane, accurate equations of state for pure *n*-heptane and isooctane are required. Speed-of-sound data form an important part of the data basis to which an equation of state is fitted because the speed of sound contains valuable information about thermal and caloric properties [8] and, thus, accurate speed-of-sound data covering a wide temperature and pressure range enable a very accurate representation of all thermodynamic properties [9]. Moreover, when supplemented by accurate density and isobaric heat capacity data at an initial isobar, all other thermodynamic properties can be derived from a speed-of-sound data set in the temperature and pressure range of the measurements by the method of thermodynamic integration [10].

The speed of sound in *n*-heptane was measured by many authors over wide temperature and pressure ranges [11–31]. However, the different data sets show considerable differences between a few tenth of a percent and several percent, and it is not known which data set is the most accurate. For the speed of sound in isooctane at high pressures, only two data sets are available in the literature. Plantier and Daridon [32] measured the speed of sound in isooctane between 293 K and 373 K with pressures up to 150 MPa, while Zhang et al. [33] measured the region between 294 K and 632 K with pressures up to 12 MPa. Since our double-path-length pulse-echo apparatus enables very accurate measurements of the speed of sound [34,35], new measurements of *n*-heptane can support to identify the most accurate among the various data sets in the literature. As our apparatus covers the temperature range between 200 K and 420 K up to 100 MPa, we can extend the temperature range over which the speed of sound in isooctane at elevated pressures is measured down to 200 K and up to 420 K. Thus, this work aims at providing accurate speed-of-sound data

* Corresponding author.
E-mail address: karsten.meier@hsu-hh.de (K. Meier).

https://doi.org/10.1016/j.fluid.2025.114432
Received 21 February 2025; Received in revised form 19 March 2025; Accepted 20 March 2025
Available online 29 March 2025

Table 1
Chemical sample description.

Chemical name	Chemical formula	CAS number	Supplier	Initial volume fraction purity	Purification method	Analysis method
n-heptane	C_7H_{16}	142-82-5	Fisher Scientific	0.999	Degassed under vacuum	Karl-Fischer titration
2,2,4-trimethylpentane (isooctane)	C_8H_{18}	540-84-1	Merck	0.998	Degassed under vacuum	Karl-Fischer titration

sets for liquid *n*-heptane and isooctane in this temperature range with pressures up to 100 MPa.

2. Experimental

The speed-of-sound instrument used in this work was described in detail by Meier [34] and Meier and Kabelac [35]. Therefore, only a brief description of the measurement principle of our speed-of-sound sensor and the apparatus is provided in the following. Our sensor employs the double-path-length pulse-echo technique. A piezoelectric quartz disk with a resonant frequency of 8 MHz is located between two stainless steel reflectors at nominal distances of about 20 mm and 30 mm from the reflector surfaces. When the crystal is excited by a sinusoidal burst signal with up to 100 cycles, it emits sound waves in both directions into the surrounding liquid. The first echoes from both reflectors arrive successively at the crystal due to the different path lengths, separated by a time difference Δt. The speed of sound w is obtained by

$$w = \frac{\Delta L}{\Delta t}, \tag{1}$$

where $\Delta L = 2(L_2 - L_1)$ is two times the difference in the distances L_2 and L_1 between the crystal and the reflector surfaces. To determine the time difference Δt very precisely, a second burst with an equal number of cycles but inverse sign and reduced amplitude is emitted. The time difference between the two emitted bursts and the amplitude of the second burst are adjusted so that the echo of the first burst from the reflector at the longer distance L_2 and the first echo of the second burst from the reflector at the shorter distance L_1 cancel each other. This cancellation is very accurately monitored on an oscilloscope, enabling a high resolution of the time difference measurement of less than one part per million. The difference in the path lengths ΔL and its temperature dependence were determined by calibration measurements with argon as described by El Hawary and Meier [1]. Reference values for the speed of sound in argon were taken from the work of Estrada-Alexanders and Trusler [36]. Changes in ΔL with temperature T and pressure p were accounted for by

$$\begin{aligned}\Delta L(T,p) = {} & \left[\Delta L(T_0, p=0) + L_c(T_0, p=0)\right] \\ & \times \left[1 + \sum_{i=1}^{4} a_i (T - T_0)^i \right. \\ & \left. - \frac{1}{E(T)}(1-2\nu)p\right] \\ & - L_c(T_0)\left[1 + \sum_{i=1}^{3} b_i (T-T_0)^i\right],\end{aligned} \tag{2}$$

where L_c is the thickness of the quartz disk, E is Young's modulus of the sensor material and ν is its Poisson ratio. The polynomials in $T - T_0$ with coefficients a_i and b_i represent the temperature dependent thermal expansion coefficients of the sensor material (stainless steel 1.4571) and quartz, respectively. The coefficients b_i were taken from the review article of Brice [37]. The value for Young's modulus of the sensor material and its temperature dependence were taken from the FEZEN database [38]. The Poisson ratio was set to $\nu = 0.3$ independent of temperature. The path difference $\Delta L(T_0, p = 0)$ at the reference temperature T_0 and zero pressure and the coefficients a_i were determined from the calibration measurements by minimizing the difference between the data of Estrada-Alexanders and Trusler [36] and the results of the calibration measurements.

The speed-of-sound sensor is installed in a pressure vessel, which is immersed in a circulating liquid bath thermostat filled with silicone oil. The thermostat sets the temperature inside the pressure vessel with a stability of 0.5 mK. The temperature is measured in the wall of the pressure vessel with a long-stem 25.5 Ω standard platinum resistance thermometer (Chino R800-2) calibrated on the International Temperature Scale of 1990 at the Physikalisch-Technische Bundesanstalt (PTB) in Berlin. Its resistance is measured by a Fluke Superthermometer 1595A bridge system with an external 25 Ω reference resistor (Tinsley 5685A). The resistor was calibrated at the PTB in Braunschweig. The expanded (coverage factor $k = 2$) uncertainty in the temperature measurement is 2.1 mK.

The pressure is measured with two nitrogen-operated Desgranges & Huot pressure balances with measurement ranges of up to 5 MPa (DH DPG5) and of up to 100 MPa (DH 5203). Both pressure balances were also calibrated at the PTB in Braunschweig. They are coupled to the sample fluid by a differential pressure null indicator (Ruska 2413). Pressures up to 5 MPa were measured with the DH DPG5 and higher pressures with the DH 5203 pressure balance. The relative expanded ($k = 2$) uncertainty in the pressure measurement amounts to 39 parts per million (ppm) above 1 MPa, is 59 ppm between 0.5 MPa and 1 MPa, and increases to 120 ppm at 0.2 MPa.

3. Materials

The *n*-heptane sample was purchased from Fisher Scientific, Germany, and had a manufacturer specified volume purity higher than 99.0%. According to the analysis of the manufacturer, the volume purity of the sample was higher than 99.9% with a water content lower than 0.007%. The isooctane sample was purchased from Merck, Germany, and had a manufacturer specified volume purity better than 99.8% with water impurities of less than 0.01%.

The samples were prepared under a nitrogen atmosphere in a glove box to avoid their contamination with ambient air. The water content of the samples was determined by Karl-Fischer titration to be 0.0029% for *n*-heptane and 0.0028% for isooctane. Since drying of the samples with molecular sieves for about twelve hours under a nitrogen atmosphere in a glove box did not reduce the water content significantly, no further attempt was made to dry the samples used for the speed-of-sound measurements. Before filling the samples into the speed-of-sound apparatus, they were degassed under vacuum multiple times to remove dissolved gases. Details of the samples are summarized in Table 1.

The contribution of sample impurities to the uncertainty in the speed-of-sound measurement was estimated with the GERG-2008 equation of state of Kunz and Wagner [39] for *n*-heptane and with the multi-fluid Helmholtz energy equation of state of Bell and Lemmon [40] for isooctane as implemented in the database REFPROP [41] individually for each measured state point. To obtain a conservative estimate for the influences of sample impurities, the second impurity beside water was assumed to be the *n*-alkane close to *n*-heptane and isooctane in the homologous series of *n*-alkanes whose presence results in the largest change in the speed-of-sound. Thus, the following impurities were assumed for the *n*-heptane sample: *n*-hexane, 0.0971%; water, 0.0029%, and the following impurities were assumed for the isooctane sample: *n*-octane, 0.1972%; water, 0.0028%. The contribution of the impurities to the uncertainty in the speed of sound measurement is between 16 ppm and 120 ppm for *n*-heptane and between 20 ppm and 300 ppm for isooctane. The largest contributions are observed near the vapor pressure at the highest measured isotherm 420 K.

Table 2
Summary of the uncertainty budget for the speed-of-sound measurement in isooctane at the state point (300 K, 50.1 MPa). All uncertainties are expanded ($k = 2$) uncertainties.

Temperature measurement:		
SPRT calibration	2.0 mK	Random
Calibration of reference resistor	0.1 mK	Random
ASL F18 bridge	0.1 mK	Random
Temperature variation in pressure vessel	0.5 mK	Random
Total uncertainty[a]	2.1 mK	
Pressure measurement: DH 5203		
Calibration of pressure balance	50×10^{-6} MPa $+ 3.2 \times 10^{-5} \cdot p + 10^{-7} \cdot p^2/\mathrm{MPa}$	Random
Differential pressure indicator	$5 \times 10^{-6} \cdot p$	Random
Hydrostatic pressure correction	$2 \times 10^{-6} \cdot p$	Random
Ambient pressure measurement	20 Pa	Random
Total uncertainty[a]	$39 \times 10^{-6} \cdot p$	
Pressure measurement: DH DPG5		
Calibration of pressure balance	2×10^{-5} MPa $+ 1.8 \times 10^{-5} \cdot p$	Random
Differential pressure indicator	$5 \times 10^{-6} \cdot p$	Random
Hydrostatic pressure correction	$2 \times 10^{-6} \cdot p$	Random
Ambient pressure measurement	20 Pa	Random
Total uncertainty[a]	$p < 0.5$ MPa: $120 \times 10^{-6} \cdot p$	
	0.5 MPa $< p < 1$ MPa: $59 \times 10^{-6} \cdot p$	
	1 MPa $< p < 5$ MPa: $39 \times 10^{-6} \cdot p$	
Determination of path length ΔL with measurements in argon:		
Time difference	$2 \times 10^{-6} \cdot \Delta L$	Random
Temperature measurement	$6 \times 10^{-6} \cdot \Delta L$	Random
Pressure measurement	$6 \times 10^{-6} \cdot \Delta L$	Random
Correction of ΔL to ambient pressure	$3 \times 10^{-6} \cdot \Delta L$	Systematic
Diffraction correction	$2 \times 10^{-6} \cdot \Delta L$	Systematic
Uncertainty of reference data	$20 \times 10^{-6} \cdot \Delta L$	Random
Mean deviation of calibration results from reference data	$20 \times 10^{-6} \cdot \Delta L$	Systematic
Total uncertainty[a]	$47 \times 10^{-6} \cdot \Delta L$	
Speed-of-sound measurement:		
Acoustic path length	$47 \times 10^{-6} \cdot c$	Random
Pressure dependence of acoustic path length	$(27 \times 10^{-8} \cdot p/\mathrm{MPa}) \cdot c$	Systematic
Time difference	$2 \times 10^{-6} \cdot c$	Random
Diffraction correction	$4 \times 10^{-6} \cdot c$	Systematic
Total uncertainty[a]	$(51 \times 10^{-6} + 25 \times 10^{-8} \cdot p/\mathrm{MPa}) \cdot c$	
Speed-of-sound measurement	$(51 \times 10^{-6} + 25 \times 10^{-8} \cdot p/\mathrm{MPa}) \cdot c$	Random
Temperature measurement	$5 \times 10^{-6} \cdot c$	Random
Pressure measurement	$6 \times 10^{-6} \cdot c$	Random
Sample impurities	$67 \times 10^{-6} \cdot c$	Systematic
Combined uncertainty in speed of sound	$131 \times 10^{-6} \cdot c$	

[a] Total uncertainties in the pressure, temperature, and speed-of-sound measurements, and the combined uncertainty in the speed-of-sound measurement were calculated by adding random contributions in quadrature and systematic contributions linearly.

4. Uncertainty budget

The uncertainty analysis for the measurements in isooctane was carried out as in our previous works, e.g. Refs. [3–5]. The uncertainty budget for the temperature, pressure, and speed-of-sound measurement is reported exemplarily for the state point (300 K, 50.1 MPa) in Table 2. Total uncertainties in the pressure, temperature, and speed-of-sound measurements and combined uncertainty in the speed-of-sound measurement, which contains the influences of the uncertainty in the temperature and pressure measurements and the influence of sample impurities, were calculated by adding random contributions in quadrature and systematic contributions linearly.

For n-heptane, some isotherms were measured up to three times with different samples from the same batch. Fig. 1 depicts relative deviations of three series of measurements at the isotherms 280 K and 300 K as examples from our speed-of-sound correlation for n-heptane described below in Section 5. It can be observed from Fig. 1 that the measurements with different samples show systematic relative differences of up to 110 ppm, while repeated measurements with the same sample after an isotherm was completed, termed reproducibility measurements in Fig. 1, agreed much better, *i.e.*, within 20 ppm. Similar observations were made for repeated measurements at other isotherms. It is assumed that these differences are caused either by small changes of the path lengths in the speed-of-sound sensor after temperature and pressure cycles or by small changes in the sample composition when filling the apparatus with a new sample. Since no unambiguous explanation for these differences could be found, the measurements of the series closest to the averages of the measurements series were taken as the final results for the isotherm. The combined expanded ($k = 2$) uncertainty in the speed of sound due to random influences was estimated by assuming that the different measurement series at each isotherm obey a Student t distribution. Thus, the random contribution to the combined expanded ($k = 2$) uncertainty in the speed-of-sound measurement was calculated by

$$U_{\mathrm{ran}} = \frac{ts}{\sqrt{n}}, \tag{3}$$

where t is Student's t factor and s is the standard deviation of n independent data points c_i from the average $\bar{c}$ given by

$$s = \sqrt{\frac{1}{n-1} \sum_{i=1}^{n} (c_i - \bar{c})^2}. \tag{4}$$

The combined ($k = 2$) uncertainty in the speed of sound is calculated by adding the random contribution, the contribution due to sample impurities, and the systematic contributions as given in Table 2 for the uncertainty budget for the isooctane measurements linearly.

5. Results

Our speed-of-sound measurements in n-heptane and isooctane were carried out along twelve isotherms between 200 K and 420 K in steps

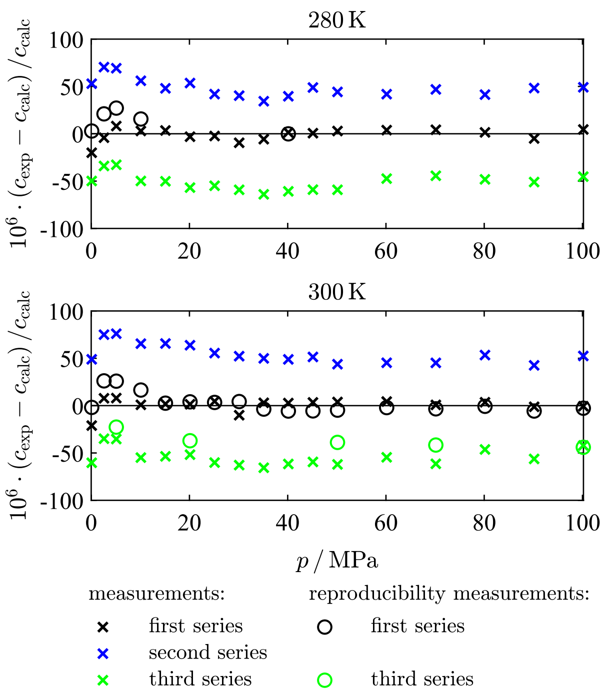

Fig. 1. Relative deviations of experimental speeds of sound c_{exp} in n-heptane for three measurement series at 280 K and 300 K from values c_{calc} calculated with our speed-of-sound correlation, Eq. (5), as a function of pressure p.

of 20 K and cover the liquid region of both fluids up to a pressure of 100 MPa. The lowest pressures at each isotherm were chosen as the atmospheric pressure near 100 kPa below the normal boiling points of n-heptane at 371.55 K and of isooctane at 372.36 K [41] and slightly above the vapor pressure above the normal boiling points between 380 K and 420 K. The distribution of our measurements and data of other authors from the literature is depicted in pressure–temperature diagrams in Fig. 2 for n-heptane and Fig. 3 for isooctane. The speed of sound in n-heptane at elevated pressures was measured by many authors before [11–31]. For isooctane, only the data set of Plantier and Daridon [32] covers elevated pressures up to 150 MPa in the temperature range between 293 K and 373 K. The data of Zhang et al. [33] cover the range from 294 K to 634 K at moderate pressures up to 12 MPa. Our measurements for isooctane extend the measured region for isooctane at elevated pressures down to 200 K and up to 420 K.

The results of our measurements for n-heptane and isooctane and their combined expanded ($k = 2$) uncertainties are reported in Tables 3 and 4. Overall, 204 state points were measured for n-heptane and 192 for isooctane. Generally, the relative expanded ($k = 2$) uncertainty in the speed of sound is less than 0.02% for n-heptane and 0.015% for isooctane. The largest uncertainties of 0.03% for n-heptane and 0.035% for isooctane are found at the state points with the lowest pressure at 420 K. For isooctane, some measurements on nine isotherms were repeated after the measurements on an isotherm were completed to check the reproducibility. These data are also reported in Table 4. They agree with the results from the main measurement campaign within their expanded ($k = 2$) uncertainty. Our measured speed-of-sound isotherms for n-heptane are depicted as a function of pressure in Fig. 4. In the measured region, the speed of sound in n-heptane varies between 632.54 m/s at about 0.4 MPa and 420 K and 1935.85 m/s at 100 MPa and 200 K. Similarly, Fig. 5 shows the measured speed-of-sound isotherms for isooctane as a function of pressure. Here, the speed of sound in the measured region ranges from 606.85 m/s at about 0.6 MPa and 420 K to 1928.63 m/s at 100 MPa and 200 K. In the measured regions of both fluids, the speed of sound decreases with temperature and increases with pressure.

For the discussion and comparison of our measurement results with data from the literature and equations of state, we developed correlations for both liquids, which represent our results for the speed of sound as a function of temperature and pressure. The functional form of the speed-of-sound correlations was determined using the linear structural optimization technique devised by Wagner [80] as adapted by El Hawary and Meier [81]. Since it was observed in our previous work [81] that a more accurate representation of the speed of sound can be obtained if the correlation is formulated for the square of the speed of sound instead of the speed of sound itself, the correlation was fitted to the former. The structural optimization started with a bank of terms that contained 1281 double polynomial terms in temperature and pressure with integer and rational exponents between 0 and 15 in steps of 0.25 for temperature and between 0 and 4 in steps of 0.2 for pressure. The optimized functional form for each fluid,

$$[c(p,T)]^2 = \sum_{i=1}^{N} a_i \left(\frac{p}{p_c}\right)^{m_i} \left(\frac{T}{T_c}\right)^{n_i}, \qquad (5)$$

consists of polynomial terms in reduced pressure and reduced temperature with integer and rational exponents, where c denotes the speed of sound in m/s, and T_c and p_c are the critical temperature and critical pressure, respectively. For n-heptane, $N = 21$ terms and for isooctane $N = 19$ terms are required to represent our data accurately. The coefficients a_i and exponents m_i and n_i for both correlations are reported in Table 5. The correlations are valid in the region of our measurements.

Fig. 6 shows relative deviations of our results for the speed of sound in n-heptane and isooctane from the correlations as functions of temperature [Figs. 6(a) and 6(c)] and pressure [Figs. 6(b) and 6(d)]. The correlation for the speed of sound in n-heptane represents our measurement results with a relative average deviation of 9 ppm and a maximum deviation of 71 ppm at 420 K and low pressure. Between 200 K and 280 K the deviations remain within 20 ppm. The correlation for isooctane represents our measurement results within 50 ppm except for one value at 380 K, one value at 400 K, and two values at 420 K, which deviate by 126 ppm, 100 ppm, 169 ppm, and 194 ppm, respectively. The relative expanded ($k = 2$) uncertainty of both correlations is estimated to be 0.02%.

6. Comparison with data of other authors from the literature

In the following, we compare our measurement results with data of other authors from the literature and the current reference equations of state for n-heptane of Tenji et al. [67] and for isooctane of Blackham et al. [79] as implemented in the NIST database REFPROP 10.0 [41]. As references for the comparison, we use the speed-of-sound correlations described in Section 5. Since many data sets for the speed of sound in n-heptane and isooctane in the literature contain only a few data points at atmospheric pressure near ambient temperature, which were mostly measured to validate benchtop instruments, we restrict the discussion to data sets which contain more than three data points. For data sets published before 1990, the reported temperatures were converted into thermodynamic temperatures on the ITS-90 using the procedures described by Harvey [82]. The literature search was carried out with the help of the NIST TDE database [83] and the Dortmund Data Bank (DDB) [84].

6.1. n-Heptane

Since the speed of sound in n-heptane was measured by many authors before, an extensive database is available. Table 6 summarizes details of these data sets, such as the measurement method, temperature and pressure ranges of the measurements, sample purity, and uncertainty of the data. Fig. 2 shows the distribution of these data sets [11,

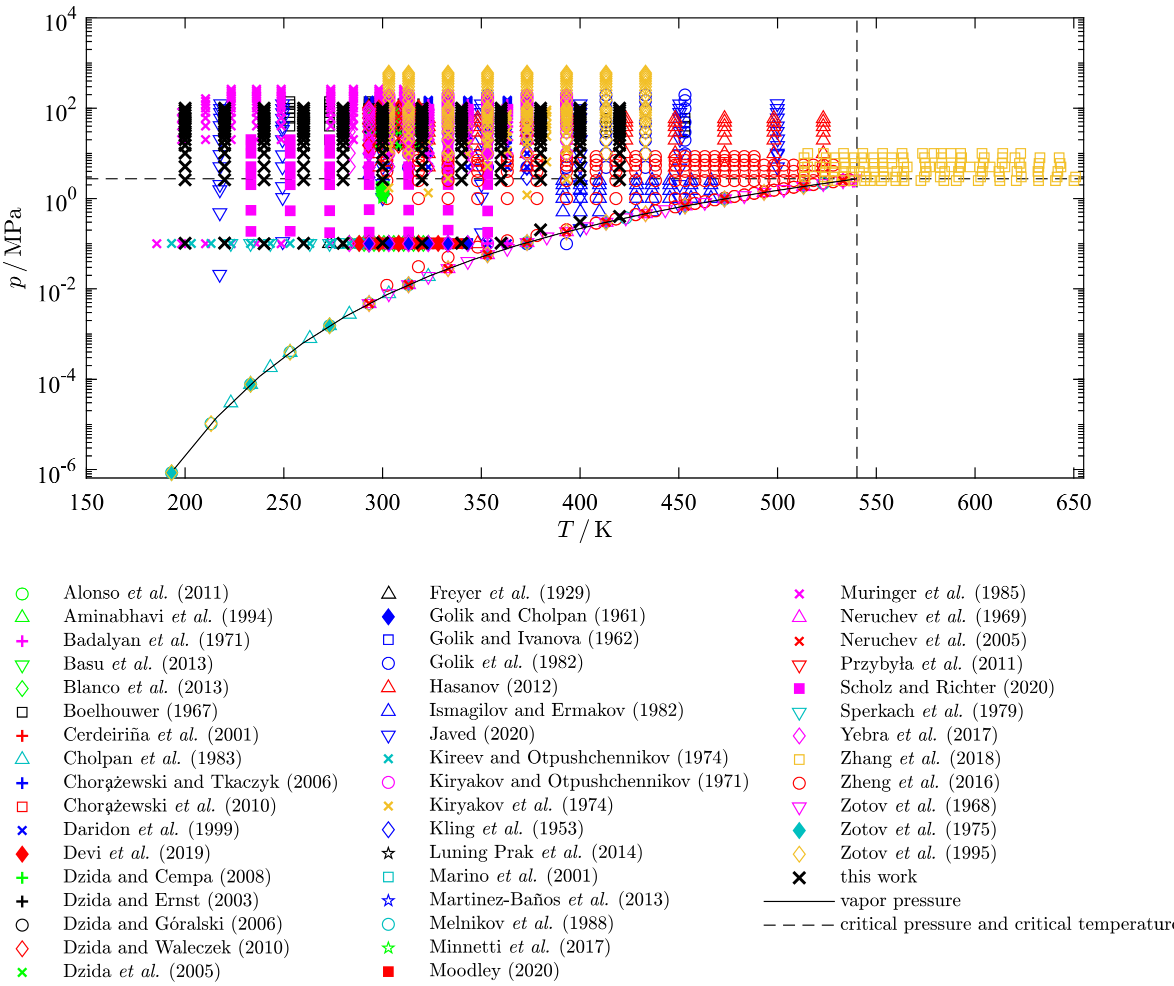

Fig. 2. Distribution of our measurements and literature data [11–31,42–66] for the speed of sound in *n*-heptane in a pressure (p)–temperature (T) diagram. The vapor pressure curve was calculated with the equation of state of Tenji et al. [67] implemented in REFPROP [41]. The critical point is at (540.2 K, 2.7357 MPa) [41].

12,16–18,20–24,30,31,42–45,48,49,52,54,56,58,85,86] in a pressure–temperature diagram. Several data sets overlap with the region of our measurements. Since the concept of standard and expanded uncertainties was not applied throughout until recently, in most cases it is not known whether the uncertainties reported by the authors are standard or expanded uncertainties. We consider all uncertainties reported in Table 6 as expanded ($k = 2$) uncertainties.

Fig. 7 shows relative deviations of our measurement results at atmospheric pressure and low pressures up to 0.4 MPa, literature data, and the equation of state of Tenji et al. [67] from our speed-of-sound correlation, Eq. (5), as a function of temperature. Above the normal boiling point, our lowest measured pressure on the measured isotherms was increased in steps of 0.1 MPa from 0.1 MPa at 360 K below the normal boiling point up to 0.4 MPa at 420 K. For the calculation of deviations of literature data that lie slightly outside our measurement range, our speed-of-sound correlation is extrapolated outside its range of validity.

The 19 data sets of Freyer et al. [52], Golik and Cholpan [53], Golik and Ivanova [54], Kireev and Otpushchennikov [55], Sperkach et al. [64], Aminabhavi et al. [43], Cerdeiriña et al. [46], Marino et al. [57], Chorążewski and Tkaczyk [48], Dzida and Góralski [23], Chorążewski et al. [49], Alonso et al. [42], Przybyła et al. [63], Basu et al. [44], Blanco et al. [45], Martinez-Baños et al. [58], Luning Prak et al. [56], Devi et al. [50], and Moodley [60] in Table 6 provide data in the temperature range between 193 K and 343 K at atmospheric pressure. The data sets of Kling et al. [11], Boelhouwer [12], Badalyan et al. [13], Kiryakov and Otpushchennikov [14] Golik et al. [16], Muringer et al. [18], Daridon et al. [20], Dzida and Ernst [21], Dzida et al. [22], Dzida and Cempa [24] Dzida and Waleczek [51] Hasanov [25] Yebra et al. [28] Javed [30], and Scholz and Richter [31] with data at elevated pressures also contain data at atmospheric or low pressure. The deviations of these data from our correlation are also included in Fig. 7.

As can be observed from Fig. 7, our data agree with most literature data at atmospheric pressures within 0.3%. The best agreement is found with the data of Boelhouwer [12] which agree with our data within 0.01% except for the value at 253 K with a deviation of −0.038%. Somewhat larger deviations of up to ±0.05% are observed for the data of Alonso et al. [42], Chorążewski and Tkaczyk [48], and Martínez-Baños et al. [58], with the data Alonso et al. [42] showing a different temperature dependence than our data. The data of Cerdeiriña et al. [46], Daridon et al. [20], Dzida and Ernst [21], Dzida and Goralski [23], Dzida et al. [22], Luning Prak et al. [56], and Javed [30] agree with our data within 0.1%. The data of Luning Prak et al. [56] also show a somewhat different temperature dependence than our data. The deviations of the data of Chorążewski et al. [49], Dzida and Cempa [24], Dzida and Waleczek [51], Przybyła et al. [63], Badalyan et al. [13], Scholz and Richter [31], and Yebra et al. [28] remain within ±0.2% except for one data point of Badalyan et al. at 303 K. All other data, *i.e.*, the data of Freyer et al. [52], Golik and Cholpan [53], Golik and Ivanova [54], Kireev and Otpushchennikov [55], Sperkach et al. [64], Aminabhavi et al. [43], Marino et al. [57], Basu et al. [44], Blanco et al. [45], Devi et al. [50], Moodley [60], Kling et al. [11], Golik et al. [16], Ismagilov and Ermakov [17], Muringer

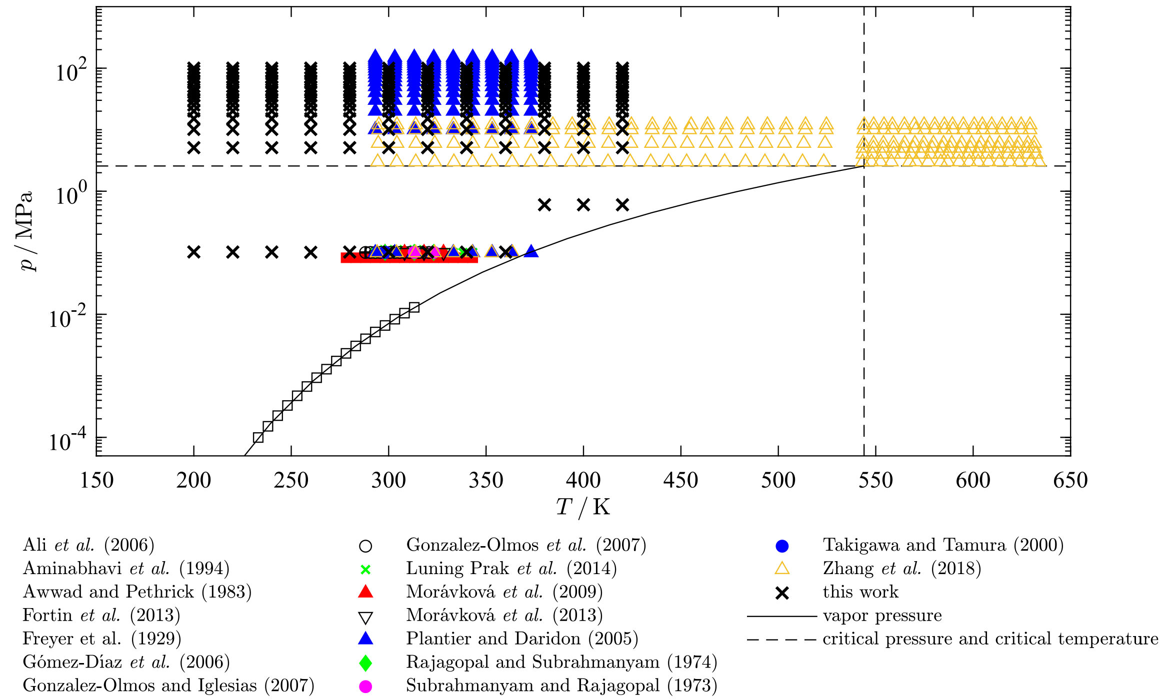

Fig. 3. Distribution of our measurements and literature data [32,33,43,52,56,68–78] for the speed of sound in isooctane in a pressure (p)–temperature (T) diagram. The vapor pressure curve was calculated with the equation of state of Blackham et al. [79] implemented in REFPROP [41]. The critical point is at (544 K, 2.572 MPa) [41].

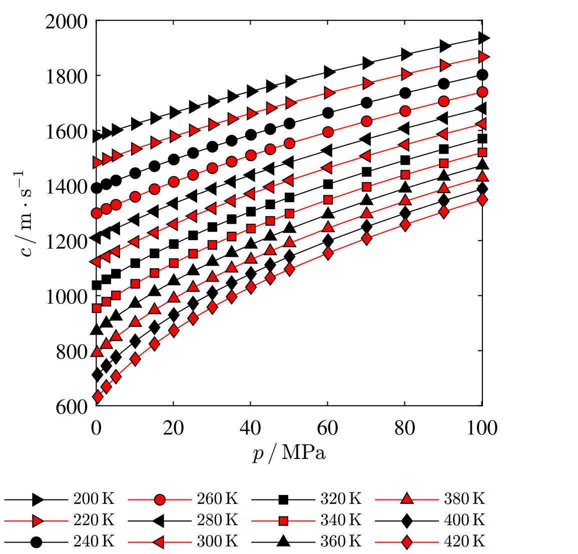

Fig. 4. Experimental results for the speed of sound c in n-heptane along isotherms as a function of pressure p.

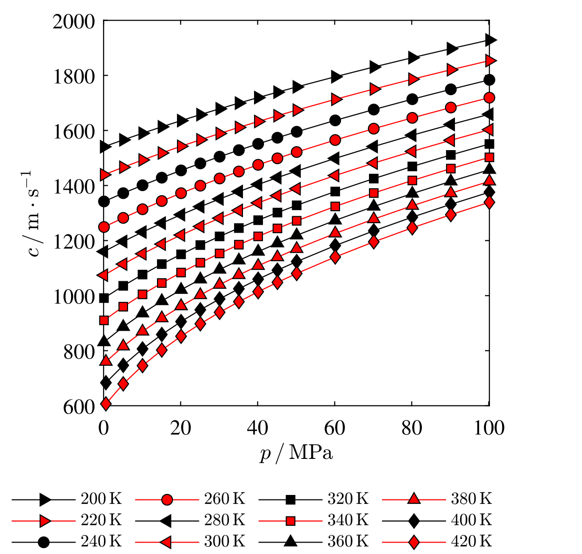

Fig. 5. Experimental results for the speed of sound c in isooctane along isotherms as a function of pressure p.

et al. [18], and Hasanov [25] show partially higher deviations from our data. The equation of state by Tenji et al. [67] agrees with our data within about 0.2%. At temperatures below 340 K the deviations are positive, while at higher temperatures the deviations become negative. At low temperatures, the equation of state follows the data of Muringer et al. [18].

Fig. 8 shows relative deviations of our measurement results at atmospheric pressure and low pressures up to 0.4 MPa and literature data at the saturated liquid line, and the equation of state of Tenji et al. [67] at the saturated liquid line from our speed-of-sound correlation, Eq. (5), as a function of temperature. Zotov et al. [65], Neruchev et al. [61], Zotov et al. [66], Cholpan et al. [47], Melnikov et al. [59], Zotov et al. [19], Neruchev et al. [62], and Zheng et al. [26] measured the speed of sound in saturated liquid or saturated vapor n-heptane. The deviations of the saturated liquid data from the speed-of-sound correlation and our data are much larger than the deviations of the most accurate literature data at atmospheric pressure, with the largest deviations amounting to between a few per mill and 0.8%. The data of Zotov et al. [65], Neruchev et al. [61], Zotov et al. [66], Melnikov et al. [59], Zotov et al. [19], and Neruchev et al. [62] exhibit a similar dependence on temperature.

Fig. 9 depicts relative deviations of our measurement results at elevated pressures, data of other authors from the literature [11–13,15–22,24–31,51], and the equation of state of Tenji et al. [67] for n-heptane from our speed-of-sound correlation along the twelve isotherms measured in this work as a function of pressure. In each

Table 3
Experimental results for the speed of sound c in n-heptane as a function of temperature T and pressure p and its combined expanded (k = 2) uncertainty $U_c(c)$.[a]

T K	p MPa	c m/s	$U_c(c)$ m/s	T K	p MPa	c m/s	$U_c(c)$ m/s
				T = 200 K			
199.9961	0.102336	1579.14	0.28	200.0042	40.1335	1742.35	0.30
199.9983	2.60563	1590.56	0.28	200.0040	45.1372	1760.39	0.30
199.9958	5.10598	1601.79	0.28	200.0048	50.1404	1778.01	0.31
199.9958	10.1096	1623.71	0.29	200.0047	60.1478	1812.11	0.31
199.9956	15.1131	1644.93	0.29	200.0041	70.1552	1844.81	0.32
199.9956	20.1169	1665.51	0.29	200.0039	80.1625	1876.27	0.32
200.0045	25.1229	1685.47	0.29	199.9995	90.1697	1906.59	0.33
199.9957	30.1243	1704.95	0.30	199.9997	100.177	1935.85	0.33
200.0041	35.1300	1723.88	0.30				
				T = 220 K			
220.0021	0.103216	1483.93	0.27	220.0018	40.1294	1661.83	0.29
220.0021	2.60501	1496.57	0.27	220.0025	45.1337	1681.20	0.29
220.0024	5.10660	1508.96	0.27	220.0019	50.1384	1700.09	0.29
220.0019	10.1099	1533.05	0.27	220.0017	60.1458	1736.52	0.30
220.0021	15.1122	1556.25	0.27	220.0022	70.1531	1771.31	0.30
220.0017	20.1144	1578.68	0.28	220.0021	80.1602	1804.65	0.31
220.0019	25.1181	1600.42	0.28	220.0022	90.1676	1836.71	0.31
220.0016	30.1217	1621.47	0.28	220.0023	100.175	1867.58	0.32
220.0016	35.1254	1641.94	0.28				
				T = 240 K			
239.9988	0.100226	1390.73	0.25	239.9999	40.1290	1584.25	0.27
239.9990	2.60167	1404.72	0.25	239.9980	45.1363	1605.01	0.28
239.9989	5.10338	1418.37	0.26	239.9987	50.1366	1625.15	0.28
239.9992	10.1067	1444.81	0.26	239.9988	60.1440	1663.89	0.29
239.9986	15.1103	1470.19	0.26	239.9986	70.1513	1700.79	0.29
239.9986	20.1143	1494.60	0.26	239.9987	80.1581	1736.02	0.30
239.9984	25.1204	1518.15	0.27	239.9986	90.1660	1769.80	0.30
239.9982	30.1243	1540.89	0.27	239.9983	100.174	1802.25	0.31
239.9996	35.1259	1562.90	0.27				
				T = 260 K			
260.0011	0.102343	1299.48	0.24	260.0020	40.1308	1509.59	0.26
260.0012	2.60421	1314.95	0.24	260.0023	45.1343	1531.70	0.27
260.0014	5.10604	1330.02	0.24	260.0024	50.1379	1553.15	0.27
260.0032	10.1092	1359.01	0.25	260.0029	60.1451	1594.25	0.27
260.0013	15.1131	1386.71	0.25	260.0027	70.1521	1633.21	0.28
260.0012	20.1168	1413.21	0.25	260.0028	80.1593	1670.32	0.29
260.0016	25.1203	1438.65	0.25	260.0029	90.1665	1705.75	0.29
260.0017	30.1237	1463.12	0.26	260.0028	100.174	1739.73	0.30
260.0018	35.1273	1486.75	0.26				
				T = 280 K			
279.9973	0.102074	1210.28	0.23	279.9962	40.1303	1438.10	0.25
279.9975	2.60372	1227.41	0.23	279.9972	45.1339	1461.60	0.26
279.9963	5.10727	1244.06	0.23	279.9970	50.1379	1484.35	0.26
279.9955	10.1083	1275.88	0.23	279.9965	60.1448	1527.77	0.26
279.9955	15.1121	1306.05	0.24	279.9972	70.1524	1568.78	0.27
279.9956	20.1159	1334.75	0.24	279.9964	80.1597	1607.70	0.28
279.9970	25.1194	1362.18	0.24	279.9968	90.1671	1644.76	0.28
279.9958	30.1233	1388.47	0.25	279.9973	100.174	1680.21	0.29
279.9972	35.1266	1413.74	0.25				
				T = 300 K			
299.9976	0.104304	1123.11	0.22	299.9978	40.1291	1369.90	0.24
299.9975	2.60597	1142.16	0.22	299.9969	45.1354	1394.83	0.25
299.9973	5.10760	1160.53	0.22	299.9974	50.1388	1418.86	0.25
299.9973	10.1109	1195.46	0.22	299.9964	60.1469	1464.60	0.26
299.9979	15.1143	1228.31	0.23	299.9962	70.1543	1507.61	0.26
299.9979	20.1175	1259.37	0.23	299.9962	80.1620	1548.29	0.27
299.9979	25.1208	1288.90	0.23	299.9961	90.1695	1586.93	0.27
299.9982	30.1240	1317.04	0.24	299.9984	100.172	1623.76	0.28
299.9982	35.1260	1344.01	0.24				
				T = 320 K			
319.9954	0.104158	1037.89	0.21	319.9959	40.1316	1305.12	0.23
319.9954	2.60593	1059.14	0.21	319.9963	45.1348	1331.44	0.24
319.9957	5.10753	1079.48	0.21	319.9967	50.1378	1356.76	0.24
319.9959	10.1108	1117.85	0.21	319.9969	60.1450	1404.76	0.25
319.9960	15.1141	1153.61	0.22	319.9970	70.1517	1449.72	0.25
319.9954	20.1179	1187.19	0.22	319.9972	80.1579	1492.11	0.26
319.9964	25.1209	1218.89	0.22	319.9976	90.1647	1532.26	0.27
319.9963	30.1241	1248.99	0.23	319.9975	100.172	1570.46	0.27
319.9968	35.1271	1277.67	0.23				

(continued on next page)

Table 3 (*continued*).

T K	p MPa	c m/s	$U_c(c)$ m/s	T K	p MPa	c m/s	$U_c(c)$ m/s
			T = 340 K				
340.0022	0.102317	954.31	0.20	340.0037	40.1281	1243.68	0.23
340.0016	2.60402	978.11	0.20	340.0040	45.1312	1271.42	0.23
340.0023	5.10570	1000.72	0.20	340.0004	50.1372	1298.05	0.23
340.0019	10.1097	1042.98	0.20	340.0009	60.1440	1348.29	0.24
340.0022	15.1126	1081.89	0.21	340.0016	70.1506	1395.15	0.25
340.0024	20.1154	1118.13	0.21	340.0022	80.1567	1439.17	0.25
340.0029	25.1187	1152.14	0.22	340.0029	90.1631	1480.77	0.26
340.0030	30.1219	1184.23	0.22	340.0029	100.170	1520.25	0.26
340.0033	35.1250	1214.68	0.22				
			T = 360 K				
360.0053	0.10274	872.10	0.19	360.0025	40.1301	1185.71	0.22
360.0046	2.60440	898.96	0.19	360.0028	45.1335	1214.86	0.22
360.0043	5.10601	924.22	0.19	360.0026	50.1372	1242.72	0.23
360.0056	10.1093	970.81	0.19	360.0032	60.1439	1295.16	0.23
359.9957	15.1126	1013.25	0.20	360.0038	70.1506	1343.86	0.24
359.9955	20.1159	1052.34	0.20	360.0044	80.1572	1389.46	0.25
359.9960	25.1191	1088.74	0.21	360.0049	90.1636	1432.44	0.25
360.0021	30.1231	1122.87	0.21	360.0053	100.170	1473.13	0.26
360.0023	35.1265	1155.11	0.21				
			T = 380 K				
379.9988	0.202726	792.03	0.18	380.0005	40.1282	1131.00	0.21
379.9987	2.60428	821.36	0.18	380.0000	45.1318	1161.55	0.21
379.9985	5.10604	849.74	0.18	380.0008	50.1348	1190.66	0.22
379.9987	10.1088	901.28	0.19	380.0016	60.1411	1245.23	0.23
379.9995	15.1119	947.48	0.19	380.0017	70.1473	1295.71	0.23
379.9983	20.1161	989.62	0.19	380.0019	80.1535	1342.83	0.24
379.9988	25.1193	1028.52	0.20	380.0019	90.1598	1387.11	0.25
379.9994	30.1222	1064.78	0.20	380.0021	100.166	1428.95	0.25
379.9999	35.1252	1098.83	0.21				
			T = 400 K				
399.9977	0.300681	712.44	0.17	399.9979	40.1279	1079.50	0.20
399.9972	2.60242	744.81	0.17	399.9995	45.1335	1111.42	0.21
399.9972	5.10403	776.95	0.17	399.9993	50.1369	1141.76	0.21
399.9976	10.1076	834.19	0.18	399.9967	60.1441	1198.41	0.22
399.9978	15.1110	884.57	0.18	399.9969	70.1512	1250.60	0.23
399.9960	20.1147	929.94	0.19	399.9982	80.1575	1299.16	0.23
399.9964	25.1179	971.44	0.19	399.9982	90.1642	1344.67	0.24
399.9967	30.1209	1009.86	0.19	399.9982	100.171	1387.60	0.25
399.9967	35.1241	1045.75	0.20				
			T = 420 K				
420.0020	0.402092	632.54	0.17	420.0022	40.1298	1031.07	0.20
420.0031	2.60423	668.79	0.17	420.0021	45.1331	1064.33	0.20
420.0015	5.10523	705.59	0.17	420.0030	50.1374	1095.85	0.20
420.0023	10.1088	769.45	0.17	420.0024	60.1437	1154.48	0.21
420.0022	15.1123	824.43	0.17	420.0033	70.1518	1208.31	0.22
420.0007	20.1166	873.24	0.18	420.0037	80.1587	1258.23	0.23
420.0012	25.1200	917.44	0.18	420.0038	90.1657	1304.90	0.23
420.0025	30.1230	958.05	0.19	420.0036	100.173	1348.85	0.24
420.0021	35.1264	995.76	0.19				

[a] Expanded ($k = 2$) uncertainty in temperature: $U(T) = 2.1$ mK; expanded ($k = 2$) uncertainty in pressure: DH DPG5: $U(p) = 120 \times 10^{-6} \cdot p$ below 0.5 MPa, $U(p) = 59 \times 10^{-6} \cdot p$ between 0.5 MPa and 1 MPa, $U(p) = 39 \times 10^{-6} \cdot p$ between 1 MPa and 5 MPa. DH 5203: $U(p) = 39 \times 10^{-6} \cdot p$.

subfigure, we include data from the literature that were measured within ±10 K of the respective isotherm. Data at low pressure that were already discussed above are not considered in Fig. 9.

Our measurement results agree best with the data of Javed [30] and Daridon et al. [20], which extend up to 125 MPa and 150 MPa, respectively. Both data sets have a relative ($k = 2$) uncertainty of 0.1%. The data of Javed agree with our results mostly within 0.025% except at 400 K, where deviations up to 0.065% are found. The data set of Daridon et al. with 279 measured state points is the most extensive of the literature data sets. These data scatter more than our results, but agree with them within 0.08%. In both cases, the agreement is within the uncertainty of the data.

The data of Scholz and Richter [31] extend up to 20 MPa and have uncertainties between 0.014% and 0.018%. They show small systematic negative deviations from our results, which increase from −0.04% at 233 K up to −0.15% at 353 K, *i.e.*, the deviations exceed the mutual uncertainties. The data of Dzida and Ernst [21], Dzida et al. [22], Dzida and Cempa [24], and Dzida and Waleczek [51] agree with our results within −0.1% to −0.15% at low pressure, but the deviations increase with pressure up to −0.48% at 100 MPa. The uncertainty in these data of 0.02%–0.05% at atmospheric pressure, 0.04%–0.09% between atmospheric pressure and 60 MPa, and 0.04%–0.07% between 60 MPa and 120 MPa thus appears to be too optimistic for large parts of the data. The data of Muringer et al. [18] extend from atmospheric pressure up to very high pressures of 263.4 MPa, and their uncertainty was reported to be 0.01%. The data are very consistent but higher than our data at low pressure by up to + 0.58%. At high pressures, the deviations decrease to below 0.08% at 100 MPa. The data of Yebra et al. [28] have an uncertainty of 0.2% and are rather consistent. With only a few exceptions, they agree with the correlation within their uncertainty.

The data of Boelhouwer [12] have a relative uncertainty of 0.1% and agree with our data mostly within their uncertainty. The data of Kling et al. [11] scatter more than our data and most of the literature data and deviate by up to 0.85% from the speed-of-sound correlation. The data of Badalyan et al. [13], Kiryakov and Otpushchennikov [14], Kiryakov et al. [15], and Golik et al. [16] also tend to scatter and agree with the correlation within 0.3%, 0.42%, 0.95%, and 0.7% respectively. The data of Zotov et al. [19] extend up to 600 MPa. Up to 100 MPa,

Table 4
Experimental data for the speed of sound c in isooctane as a function of temperature T and pressure p and its combined expanded (k = 2) uncertainty $U_c(c)$.[a].

T K	p MPa	c m/s	$U_c(c)$ m/s	T K	p MPa	c m/s	$U_c(c)$ m/s
			T = 200 K				
199.9969	0.103131	1540.90	0.20	199.9971	40.1283	1719.46	0.19
199.9966	5.10668	1565.85	0.20	199.9974	45.1314	1739.05	0.18
199.9971	10.1095	1589.92	0.20	199.9972	50.1345	1758.17	0.18
199.9972	15.1126	1613.17	0.19	199.9973	60.1409	1795.10	0.19
199.9970	20.1157	1635.68	0.19	199.9975	70.1473	1830.46	0.19
199.9970	25.1189	1657.52	0.19	199.9969	80.1540	1864.41	0.19
199.9968	30.1219	1678.75	0.19	199.9970	90.1604	1897.09	0.19
199.9971	35.1251	1699.38	0.19	199.9973	100.167	1928.63	0.19
			T = 220 K				
220.0008	0.102662	1439.06	0.20	220.0004	40.1293	1632.59	0.19
219.9984	0.101882	1439.11	0.20[b]	220.0006	45.1324	1653.49	0.19
220.0010	5.10274	1466.47	0.20	220.0005	50.1356	1673.84	0.18
220.0014	10.1093	1492.82	0.20	219.9988	50.1351	1673.86	0.18[b]
219.9984	10.1085	1492.86	0.20[b]	220.0003	60.1420	1713.03	0.18
220.0005	15.1125	1518.13	0.20	220.0006	70.1484	1750.41	0.19
220.0006	20.1158	1542.55	0.19	220.0005	80.1548	1786.17	0.19
220.0006	25.1190	1566.13	0.19	220.0004	90.1611	1820.51	0.19
220.0007	30.1222	1588.95	0.19	220.0004	100.167	1853.54	0.19
220.0003	35.1260	1611.10	0.19				
			T = 240 K				
239.9983	0.102733	1342.07	0.21	239.9986	45.1318	1573.60	0.18
239.9972	0.102992	1342.13	0.21[b]	239.9986	50.1351	1595.22	0.18
239.9986	5.10389	1372.21	0.20	239.9975	50.1353	1595.16	0.18[b]
239.9984	10.1090	1400.98	0.20	239.9985	60.1415	1636.56	0.19
239.9972	10.1095	1401.03	0.20[b]	239.9970	60.1414	1636.62	0.19[b]
239.9984	15.1121	1428.48	0.19	239.9991	70.1481	1675.92	0.19
239.9983	20.1152	1454.89	0.19	239.9974	70.1479	1675.92	0.19[b]
239.9983	25.1184	1480.29	0.19	239.9985	80.1545	1713.59	0.19
239.9985	30.1221	1504.76	0.19	239.9988	90.1610	1749.41	0.19
239.9986	35.1253	1528.44	0.19	239.9987	100.168	1783.85	0.19
239.9984	40.1286	1551.38	0.19				
			T = 260 K				
260.0044	0.101574	1249.22	0.21	260.0046	35.1244	1450.86	0.19
260.0021	0.102304	1249.30	0.21[b]	260.0050	40.1277	1475.19	0.19
260.0047	5.10216	1282.37	0.20	260.0049	45.1309	1498.79	0.19
260.0044	10.1079	1313.81	0.20	260.0046	50.1341	1521.62	0.19
260.0024	10.1087	1313.85	0.20[b]	260.0054	60.1407	1565.20	0.19
260.0048	15.1111	1343.64	0.19	260.0050	70.1480	1606.50	0.19
260.0050	20.1147	1372.12	0.19	260.0049	80.1544	1645.76	0.19
260.0048	25.1180	1399.40	0.19	260.0054	90.1608	1683.25	0.19
260.0053	30.1212	1425.60	0.19	260.0051	100.167	1719.13	0.20
260.0008	30.1217	1425.64	0.19[b]				
			T = 280 K				
280.0009	0.102675	1160.13	0.21	280.0015	35.1255	1378.05	0.19
280.0020	0.102613	1160.20	0.21[b]	280.0013	40.1287	1403.86	0.18
280.0010	5.10323	1196.66	0.20	280.0011	45.1319	1428.74	0.18
280.0006	10.1083	1230.96	0.20	280.0007	50.1351	1452.80	0.18
280.0020	10.1092	1231.06	0.20[b]	280.0004	60.1415	1498.61	0.19
280.0007	15.1112	1263.33	0.19	280.0010	70.1477	1541.76	0.19
280.0016	20.1158	1294.00	0.19	280.0009	80.1541	1582.77	0.19
280.0021	25.1190	1323.24	0.19	280.0009	90.1605	1621.72	0.19
280.0005	30.1222	1351.22	0.19	280.0009	100.167	1658.95	0.20
280.0023	30.1222	1351.25	0.19[b]				
			T = 300 K				
300.0017	0.103075	1074.24	0.21	300.0011	40.1274	1336.93	0.18
300.0010	5.10594	1114.55	0.20	300.0023	45.1303	1363.15	0.18
300.0022	10.1087	1152.00	0.19	300.0018	50.1332	1388.37	0.18
300.0017	15.1118	1187.09	0.19	300.0018	60.1401	1436.41	0.18
300.0009	20.1150	1220.10	0.19	300.0016	70.1465	1481.49	0.18
300.0007	25.1183	1251.40	0.19	300.0021	80.1526	1524.05	0.19
300.0007	30.1213	1281.20	0.18	300.0019	90.1590	1564.45	0.19
300.0010	35.1243	1309.65	0.18	300.0015	100.165	1602.95	0.19
			T = 320 K				
319.9982	0.102885	991.03	0.21	319.9979	30.1227	1215.16	0.18
320.0012	0.103519	991.12	0.21[b]	320.0016	35.1256	1245.41	0.18
319.9984	5.10258	1035.57	0.20	319.9984	40.1288	1274.05	0.18
319.9980	10.1095	1076.55	0.19	320.0019	45.1319	1301.73	0.18
320.0012	10.1088	1076.66	0.19[b]	319.9981	50.1355	1328.09	0.18
320.0015	10.1096	1076.70	0.19[b]	319.9979	60.1423	1378.24	0.18
319.9982	15.1128	1114.52	0.19	319.9980	70.1489	1425.12	0.18

(continued on next page)

Table 4 (*continued*).

T K	p MPa	c m/s	$U_c(c)$ m/s	T K	p MPa	c m/s	$U_c(c)$ m/s
320.0012	15.1120	1114.61	0.19[b]	320.0026	80.1547	1469.33	0.18
319.9978	20.1161	1150.03	0.18	320.0025	90.1612	1511.13	0.19
320.0016	25.1193	1183.60	0.18	320.0027	100.168	1550.84	0.19
			T = 340 K				
339.9970	0.102383	910.17	0.21	340.0001	35.1252	1184.99	0.17
340.0000	0.102736	910.24	0.21[b]	339.9976	40.1287	1215.21	0.17
339.9973	5.10246	959.75	0.20	340.0000	45.1318	1244.16	0.17
339.9975	10.1089	1004.63	0.19	339.9976	50.1352	1271.80	0.17
339.9998	10.1089	1004.71	0.19[b]	339.9999	50.1354	1271.84	0.17[b]
340.0014	10.1095	1004.69	0.19[b]	340.0021	50.1358	1271.84	0.17[b]
339.9974	15.1122	1045.74	0.18	339.9971	60.1417	1324.02	0.17
339.9974	20.1157	1083.87	0.18	339.9972	70.1482	1372.66	0.17
339.9998	25.1187	1119.61	0.18	340.0018	80.1555	1418.35	0.18
340.0019	25.1194	1119.60	0.18[b]	340.0019	90.1621	1461.44	0.18
339.9975	30.1223	1153.13	0.17	340.0020	100.169	1502.34	0.18
			T = 360 K				
360.0033	0.102487	831.20	0.21	360.0050	40.1271	1160.05	0.17
360.0032	5.10206	886.60	0.19	360.0041	45.1318	1190.24	0.17
360.0034	10.1086	935.81	0.19	360.0060	50.1324	1219.11	0.17
360.0032	10.1090	935.79	0.19[b]	360.0043	50.1351	1219.10	0.17[b]
359.9971	10.1096	935.87	0.19[b]	359.9970	50.1357	1219.15	0.17[b]
360.0032	15.1117	980.33	0.18	360.0061	60.1377	1273.36	0.17
360.0027	20.1150	1021.23	0.17	360.0068	70.1429	1323.72	0.17
360.0034	25.1188	1059.20	0.17	360.0062	80.1483	1370.78	0.17
360.0047	30.1212	1094.78	0.17	360.0056	90.1543	1415.14	0.17
360.0037	35.1253	1128.27	0.17	359.9971	100.168	1457.19	0.18
			T = 380 K				
379.9971	0.603020	760.03	0.21	379.9962	35.1254	1075.02	0.16
379.9961	0.603202	760.02	0.21[b]	379.9955	40.1289	1108.25	0.16
379.9971	5.10424	815.79	0.19	379.9965	45.1318	1139.75	0.16
379.9966	10.1087	869.82	0.18	379.9953	50.1353	1169.80	0.16
379.9959	10.1091	869.84	0.18[b]	379.9957	60.1417	1226.03	0.16
379.9961	15.1120	918.04	0.17	379.9959	70.1484	1278.01	0.16
379.9962	20.1152	961.86	0.17	379.9955	80.1549	1326.49	0.16
379.9962	20.1156	961.89	0.17	379.9954	90.1614	1372.04	0.17
379.9959	25.1189	1002.26	0.17	379.9953	100.168	1415.06	0.17
379.9959	30.1217	1039.78	0.16				
			T = 400 K				
399.9960	0.602789	683.57	0.21	399.9970	35.1251	1024.95	0.15
399.9965	0.602559	683.57	0.21[b]	399.9955	40.1284	1059.64	0.15
399.9963	5.10631	746.77	0.19	399.9973	45.1316	1092.45	0.15
399.9960	10.1087	806.45	0.18	399.9964	50.1348	1123.59	0.15
399.9964	10.1088	806.46	0.18[b]	399.9975	50.1352	1123.59	0.15[b]
399.9960	15.1119	858.70	0.17	399.9964	60.1413	1181.74	0.15
399.9962	20.1151	905.61	0.16	399.9964	70.1480	1235.30	0.16
399.9969	20.1154	905.62	0.16[b]	399.9960	80.1546	1285.09	0.16
399.9973	25.1186	948.44	0.16	399.9963	90.1612	1331.75	0.16
399.9958	30.1215	988.02	0.16	399.9965	100.168	1375.76	0.17
			T = 420 K				
419.9984	0.602039	606.86	0.21	419.9992	40.1285	1014.09	0.15
419.9985	5.10201	679.41	0.19	419.9986	45.1318	1048.14	0.15
419.9981	10.1085	745.61	0.17	419.9990	50.1354	1080.38	0.15
419.9977	15.1118	802.22	0.16	419.9990	60.1416	1140.33	0.15
419.9987	20.1155	852.35	0.16	419.9993	70.1480	1195.36	0.15
419.9991	25.1187	897.70	0.15	419.9994	80.1545	1246.40	0.15
419.9989	30.1221	939.34	0.15	419.9988	90.1610	1294.13	0.16
419.9992	35.1252	977.95	0.15	419.9986	100.168	1339.04	0.16

[a] Expanded ($k = 2$) uncertainty in temperature: $U(T) = 2.1$ mK; expanded ($k = 2$) uncertainty in pressure: DH DPG5: $U(p) = 120 \times 10^{-6} \cdot p$ below 0.5 MPa, $U(p) = 59 \times 10^{-6} \cdot p$ between 0.5 MPa and 1 MPa, $U(p) = 39 \times 10^{-6} \cdot p$ between 1 MPa and 5 MPa. DH 5203: $U(p) = 39 \times 10^{-6} \cdot p$.

[b] Reproducibility measurement.

they agree with the correlation with a few exceptions within 0.4%. The data of Ismagilov and Ermakov [17] were partially measured in the superheated liquid and deviate from the correlation by up to 2%. The data of Hasanov [25] and Zheng et al. [26] deviate in large parts by much more than 0.4% from the correlation and are therefore not shown in the plots. Minnetti et al. [27] measured only a small pressure range between 1 MPa and 2.15 MPa at 300 K. Their data agree with the correlation within 0.12% but exhibit a different dependence on pressure than our data.

The equation of state of Tenji et al. [67] agrees best with our data between 380 K and 420 K at pressures above 20 MPa. The deviations in this region are within 0.05%. The highest deviations from our results are observed at low pressure, where they amount to between −0.19% at 420 K and +0.22% at 220 K. At high pressure, the deviations increase with decreasing temperature and reach the maximum of −0.1% at 240 K.

6.2. Isooctane

Table 7 summarizes details of selected data sets for the speed of sound in isooctane from other authors in the literature, and Fig. 3 illustrates the distribution of these data sets in a pressure–temperature diagram. Only Plantier and Daridon [32] and Zhang et al. [33] measured the speed of sound at high pressures. The data of Plantier and

Table 5
Coefficients a_i and exponents m_i and n_i in the speed-of-sound correlations, Eq. (5), for *n*-heptane and isooctane.

i	*n*-heptane			isooctane		
	a_i	m_i	n_i	a_i	m_i	n_i
1	$1.489965730 \times 10^{6}$	0.00	0.00	$-3.015099849 \times 10^{2}$	−5.00	0.0
2	$1.322262719 \times 10^{4}$	1.25	0.00	$-1.376416106 \times 10^{1}$	−3.50	1.0
3	$6.893908093 \times 10^{1}$	2.00	0.00	$1.009422076 \times 10^{6}$	−1.00	0.0
4	$-5.895265731 \times 10^{3}$	1.50	0.25	$-1.589543775 \times 10^{1}$	−0.80	2.0
5	$-8.680369723 \times 10^{6}$	0.00	−0.75	$1.938594264 \times 10^{3}$	−0.20	1.5
6	$4.899614043 \times 10^{4}$	1.00	0.75	$4.769636521 \times 10^{4}$	0.20	1.0
7	$4.354578659 \times 10^{4}$	0.75	1.00	$-3.770917812 \times 10^{3}$	0.20	1.5
8	$1.809782837 \times 10^{7}$	0.00	−1.50	$2.836325441 \times 10^{4}$	1.90	1.0
9	$-5.517459563 \times 10^{5}$	0.75	2.75	$-2.009795643 \times 10^{4}$	2.10	0.5
10	$2.200573141 \times 10^{4}$	1.50	2.75	$0.030456338 \times 10^{0}$	2.40	4.0
11	$5.307956253 \times 10^{5}$	0.75	3.00	$-6.157609592 \times 10^{3}$	2.80	1.5
12	$-2.809739166 \times 10^{0}$	3.50	3.25	$-3.356051438 \times 10^{8}$	4.00	0.0
13	$5.448901367 \times 10^{4}$	0.00	−3.50	$1.916690685 \times 10^{9}$	4.50	0.0
14	$-3.273036669 \times 10^{4}$	1.75	3.50	$-3.968422900 \times 10^{3}$	4.70	1.5
15	$1.208897452 \times 10^{4}$	1.25	4.00	$3.136520969 \times 10^{2}$	4.70	2.5
16	$7.575339510 \times 10^{3}$	2.50	4.00	$-2.515340681 \times 10^{9}$	4.75	0.0
17	$-1.978587309 \times 10^{4}$	2.50	4.25	$-2.967821692 \times 10^{1}$	4.90	3.0
18	$1.709297400 \times 10^{3}$	2.75	4.25	$9.332562015 \times 10^{8}$	5.00	0.0
19	$2.992369346 \times 10^{4}$	2.25	4.50	$3.685934389 \times 10^{4}$	5.00	0.5
20	$-1.622257646 \times 10^{4}$	2.00	5.00			
21	$-1.103734320 \times 10^{7}$	0.00	−1.75			

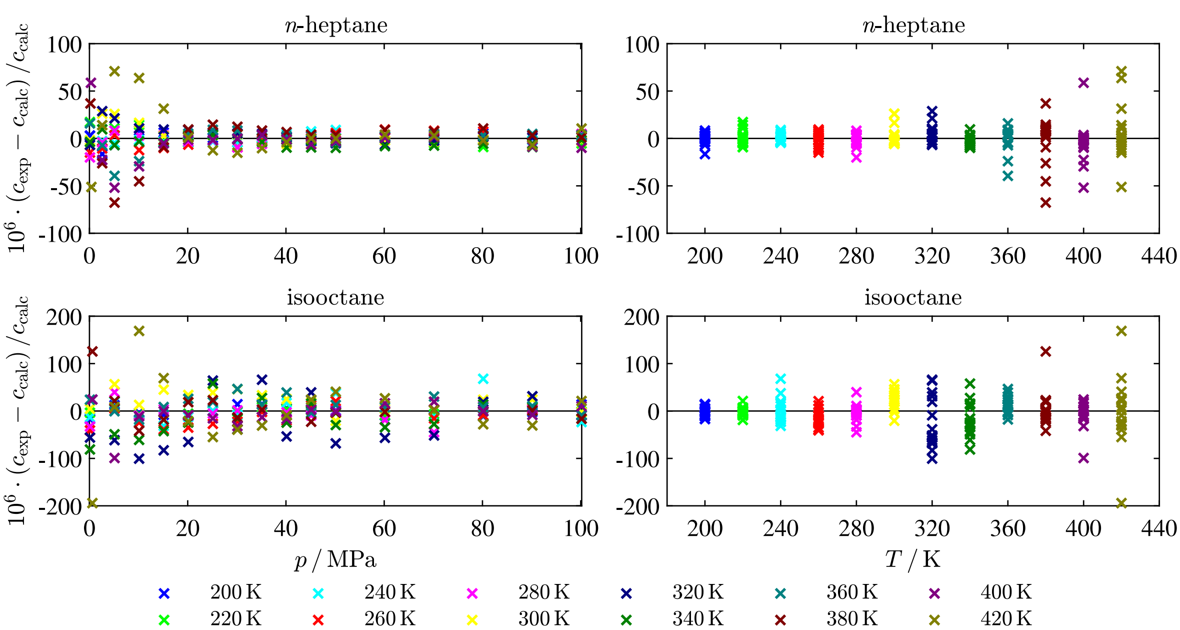

Fig. 6. Relative deviations of our experimental speeds of sound c_{exp} in *n*-heptane (top) and isooctane (bottom) from values c_{calc} calculated with the speed-of-sound correlations, Eq. (5), as a function of pressure p (left) and temperature T (right).

Daridon cover the temperature range between 293 K and 373 K with elevated pressures up to 150 MPa, while the data of Zhang et al. cover the temperature range from 294 K to 634 K with moderate pressures up to 12 MPa. Both data sets overlap with the region of our measurements. Awwad and Pethrick [69] measured the speed of sound in saturated liquid isooctane between 233 K and 313 K. All other authors, *i.e.*, Ali et al. [68], Aminabhavi et al. [43], Fortin et al. [70], Freyer et al. [52], Gómez-Días et al. [71], Gonzales-Olmos and Iglesias [73], Gonzales-Olmos et al. [72], Luning Prak et al. [56], Morávková et al. [74], Morávková et al. [75], Rajagopal and Subrahmanyam [76], Subrahmanyam and Rajagopal [77], and Takigawa and Tamura [78] measured the speed of sound at atmospheric pressure.

Fig. 10 shows relative deviations of our measurement results at atmospheric pressure, the literature data at atmospheric pressure, and the equation of state of Blackham et al. [79] for isooctane from our speed-of-sound correlation as a function of temperature. The data of Gómez-Diaz et al. [71], Gonzales-Olmos and Iglesias [72], Gonzales-Olmos et al. [73], Morávková et al. [74], Fortin et al. [70], Morávková et al. [75], and Subrahmanyam and Rajagopal [77] are very consistent and exhibit a similar temperature dependence. The data of Morávková et al. are 0.05% and the data of Fortin et al. are 0.15% higher than the other data. Except for the data of Subrahmanyam and Rajagopal, these data sets were measured with a commercial Anton Paar DSA 5000 M density and sound speed analyzer. The data of Fortin et al. were measured at an atmospheric pressure of 83 kPa, while the other data were measured at 101.325 kPa. However, such a small difference in pressure does not explain the deviation of 0.15% between the data sets. These data sets agree best with our results between 280 K and 300 K, but show negative deviations at lower temperatures, and, at higher temperatures, the deviations from our results are positive and increase.

The value measured by Freyer et al. [52] at 318 K agrees with our results within 0.02% and the data of Takigawa and Tamura [78] at

Table 6
Details of selected literature data sets for the speed of sound in liquid *n*-heptane.

Author	Year	Method[a]	f/MHz	Purity/%	Data points	T/K	p/MPa	$U_r(c)$/%
Liquid at atmospheric pressure								
Freyer et al. [52]	1929	IF	0.414	n.r.	7	273–323		0.01
Golik and Cholpan [53]	1961	IF	4	n.r.	6	293–343		0.2
Golik and Ivanova [54]	1962	IF	4	n.r.	6	293–343		n.r.
Kireev and Otpushchennikov [55]	1974	PE	1–3	n.r.	12	193–303		0.3
Sperkach et al. [64]	1979	PM	10–130	n.r.	7	223–323		0.5
Aminabhavi et al. [43]	1994	IF		99.5	5	298–318		0.2
Cerdeiriña et al. [46]	2001	DSA-48		99.5	42	288–329		0.1
Marino et al. [57]	2001	DSA-48		99.5	6	278–298		0.05
Chorążewski and Tkaczyk [48]	2006	PE	4	99.8	5	293–315		0.01
Dzida and Góralski [23]	2006	PE	n.r.	99.8	6	293–318		0.05
Chorążewski et al. [49]	2010	PE	4	99.8	5	293–313		0.05
Alonso et al. [42]	2011	DSA-48		99.0	7	283–313		0.01
Przybyła et al. [63]	2011	PE	4	99.0	5	293–313		0.05
Basu et al. [44]	2013	DSA		99.5	6	298–323		0.07
Blanco et al. [45]	2013	DSA-48		99.5	15	288–323		0.03
Martínez-Baños et al. [58]	2013	DSA		99.5	10	293–313		0.1
Luning Prak et al. [56]	2014	DSA		99.9	10	293–338		0.05
Devi et al. [50]	2019	DSA		99.7	11	288–328		0.001
Moodley [60]	2020	DSA		99.9	5	298–338		0.2
Saturated liquid								
Zotov et al. [65]	1968	PM	1	n.r.	27	293–539		0.2–2.6
Neruchev et al. [61]	1969	PE	1	n.r.	13	293–533		0.17–1.6
Zotov et al. [66]	1975	TOF	1	n.r.	10	193–513		0.1–1.3
Cholpan et al. [47]	1983	PM	10	n.r.	11	223–323		0.1
Melnikov et al. [59]	1988	PM	n.r.	n.r.	11	193–524		0.2
Zotov et al. [19]	1995	PM	1–3.5	n.r.	6	233–453		0.2–0.4
Neruchev et al. [62]	2005	PM	1–5	n.r.	35	193–553		0.1–1.0
Zheng et al. [26]	2016	LS	–	99.0	30	302–536		1.6
Liquid at elevated pressures								
Kling et al. [11]	1953	DF	n.r.	n.r.	23	293–373	0.1–49.03	0.3
Boelhouwer [12]	1967	PE	2	99.6	54	253–453	0.1–140.1	0.1
Badalyan et al. [13]	1971	TOF	2	n.r.	91	303–363	0.1—117.78	0.25
Kiryakov and Otpushchennikov [14]	1971		n.r.	n.r.	123	303–394	0.1–203	n.r.
Kiryakov et al. [15]	1974				54	303–393	1.21–99.16	
Golik et al. [16]	1982	PE	n.r.	n.r.	68	313–453	0.1–196	0.3
Ismagilov and Ermakov (superheated) [17]	1982	PE	2.5	n.r.	48	391–466	0–2.53	0.5
Muringer et al. [18]	1985	PE	2	n.r.	113	186–311	0.1–263.37	0.01
Zotov et al. [19]	1995	PM	1–3.5	n.r.	18	313–413	20–100	0.2–0.4
Daridon et al. [20]	1999	PE	3	99.5	279	293–373	0.1–150	0.1
Dzida and Ernst [21]	2003	PE	4	99.5	59	293–318	0.1–121.58	0.03–0.05
Dzida et al. [22]	2005	PE	4	99.5	88	293–318	0.1–92.07	0.04–0.05
Dzida and Cempa [24]	2008	PE	2	99.0	69	293–318	0.1–101.32	0.05–0.09
Dzida and Waleczek [51]	2010	PE	4	99.0	48	293–318	0.1–101.32	0.05–0.09
Hasanov [25]	2012	PE	8	99.98	73	298–523	0.1–58.9	0.2
Zheng et al. [26]	2016	LS	–	99.0	136	302–528	1.0–8.5	1.6
Minnetti et al. [27]	2017	PE	4	n.r.	20	300	1.03–2.13	0.3
Yebra et al. [28]	2017	TOF	1.5	99	84	283–343	0.1–95.1	0.2
Zhang et al. [29]	2018	LS	–	99	124	513–651	2.5–10	1.3
Javed [30]	2020	PE	8	n.r.	82	218–500	0.02–125.35	0.015–0.03
Scholz and Richter [31]	2021	PE	8	99.84	56	233–353	0.18–20.19	0.014–0.018
This work	2025	PE	8	99.9	204	200–420	0.1–100.1	0.02

[a] Abbreviations: DF: Diffraction of light by ultrasonic waves, DSA: densimeter and sound analyzer DSA 5000 M, IF: interferometer, n.r.: not reported, PE: pulse-echo method, PM: pulse-phase method, LS: light scattering, SA: sing-around method, SFAR: swept frequency acoustic resonator, SI: secondary interference, TOF: time-of-flight method.

293 K within 0.1%, whereas the data of Aminabhavi et al. [43], Awwad and Pethrick [69], and Plantier and Daridon [32] scatter more than all other data and show larger deviations up to 0.26%. However, the temperature dependence of the data of Awwad and Pethrick [69] and Plantier and Daridon [32] is similar to that of our results. The data of Zhang et al. [33] agree up to 353 K with our results within 0.18%, while the value at 364 K deviates by 0.57%.

Meier and Kabelac [87] measured the speed of sound in liquid toluene with the same apparatus that was used in this work and compared their results to data for toluene obtained by Fortin et al. [70] with an Anton Paar DSA 5000 M sound analyzer. They found similar differences between the two data sets as those observed in this work for isooctane. These differences are probably due to the calibration procedure of the DSA 5000 M sound analyzer. The acoustic path length in the speed-of-sound sensor of the DSA 5000 M is calibrated only at a single temperature, usually at 293.15 K, whereas we calibrate the acoustic path length in our sensor over the whole temperature range of the measurements. Thus, the temperature dependence of the data from the literature measured with a DSA 5000 M sound analyzer is probably not correct and due to an insufficient calibration of the instrument.

Fig. 11 depicts relative deviations of our measurement results at elevated pressures, data of Plantier and Daridon [32] and Zhang et al. [33] at nearby temperatures within ±10 K of our measured isotherms, and the equation of state of Blackham et al. [79] from our speed-of-sound correlation for isooctane along all measured isotherms as a function of pressure. The data of Plantier and Daridon [32] exhibit the same pressure dependence as our results and agree with them mostly within 0.1%, *i.e.*, within their uncertainty of 0.12%. For most of the data, the deviations from our results are positive. Only a few data points at low pressure show deviations of up to 0.2%. The data of Zhang et al. scatter more than our data and the data of Plantier and Daridon, lie partially outside the scale of the plots, and deviate from the correlation by up to 0.78%. The equation of state of Blackham et al. shows larger deviations from our results than the data of Plantier and Daridon [32]. The largest

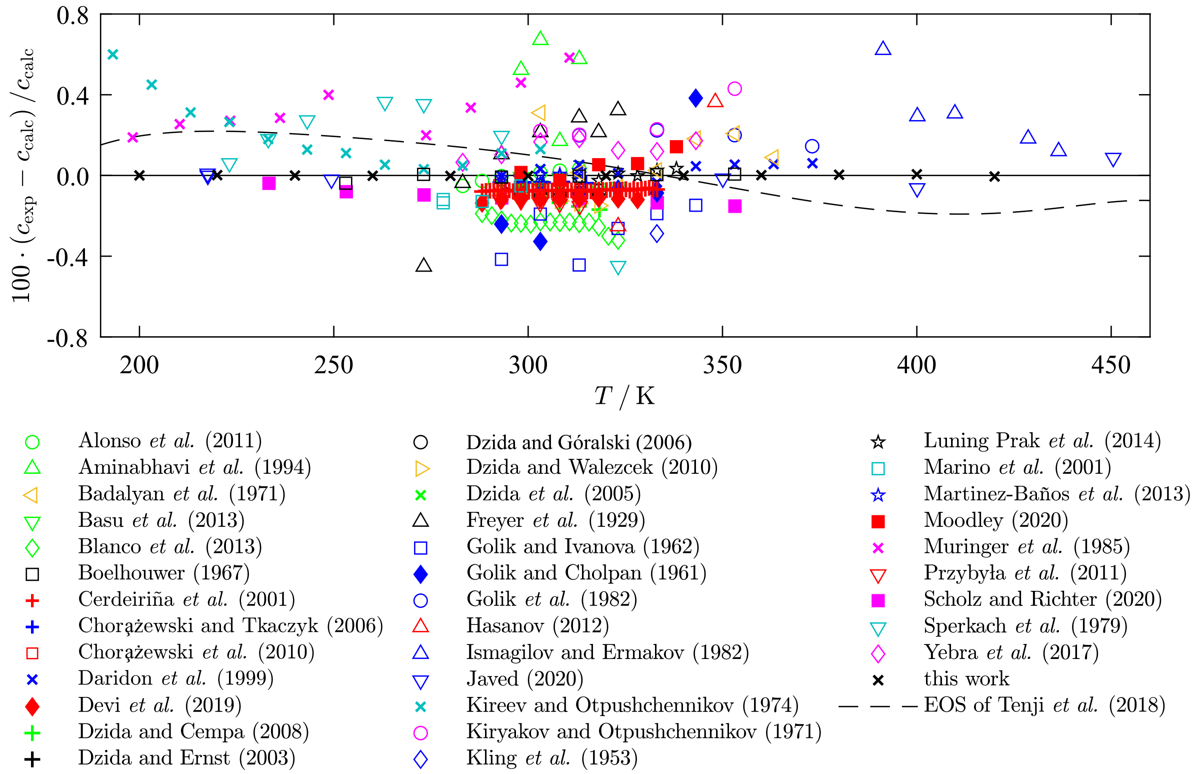

Fig. 7. Relative deviations of our experimental speeds of sound c_{exp} in n-heptane at ambient pressure, data of other authors from the literature [11–14,16–18,20–25,28,30,31,42–46,48–58,60,63,64], and the equation of state of Tenji et al. [67] implemented in REFPROP [41] from values c_{calc} calculated with our speed-of-sound correlation, Eq. (5), as a function of temperature T. Above the normal boiling point of n-heptane at 371.55 K, deviations of our results at pressures slightly above the vapor pressure are shown.

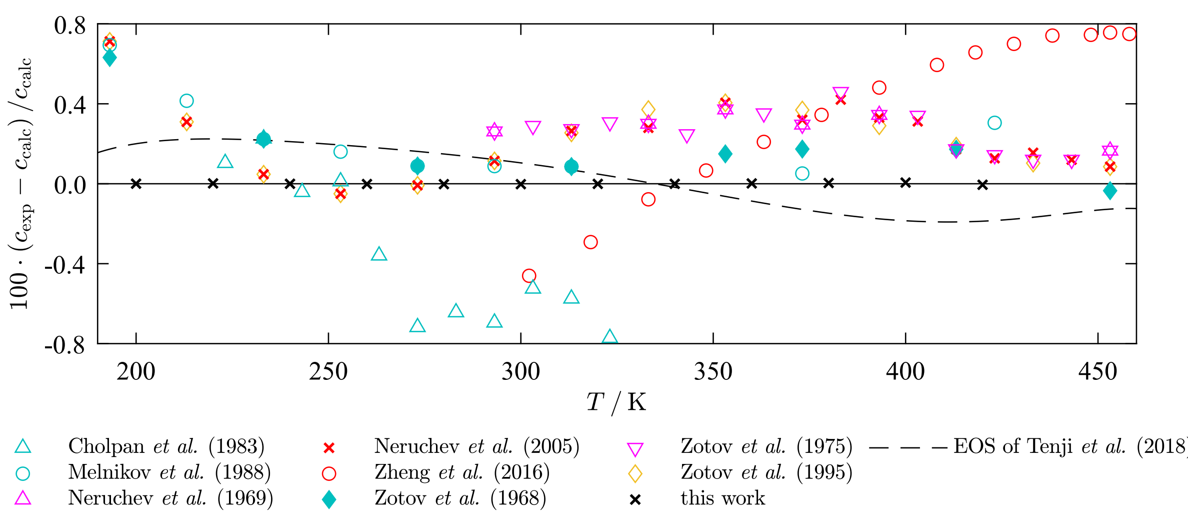

Fig. 8. Relative deviations of our experimental speeds of sound c_{exp} in n-heptane at atmospheric pressure and data of other authors from the literature [19,26,47,59,61,62,65,66] and the equation of state of Tenji et al. [67] implemented in REFPROP [41] at the saturated liquid line from values c_{calc} calculated with our speed-of-sound correlation, Eq. (5), as a function of temperature T. Above the normal boiling point of n-heptane at 371.55 K, deviations of our results at pressures slightly above the vapor pressure are shown.

deviation amounts to −0.18% at 200 K, decreases to −0.05% at 240 K, and increases again to up to + 0.45% at 420 K.

7. Conclusions

We performed accurate speed-of-sound measurements in pure n-heptane and isooctane in the liquid region between 200 K and 420 K with pressures up to 100 MPa. Our results have a lower uncertainty and are more consistent than the available speed-of-sound data sets of other authors in the literature. The measurements for isooctane extend the temperature range in which the speed of sound in isooctane has been measured down to 200 K and up to 420 K. Our data can be used to develop new, more accurate equations of state for n-heptane and isooctane with lower uncertainties not only in the speed of sound but also for other properties, such as the density and the isochoric and isobaric heat capacity, than those of the present reference equations of state for both fluids. Moreover, we observed that data of other authors from the literature at ambient pressure, which were measured with

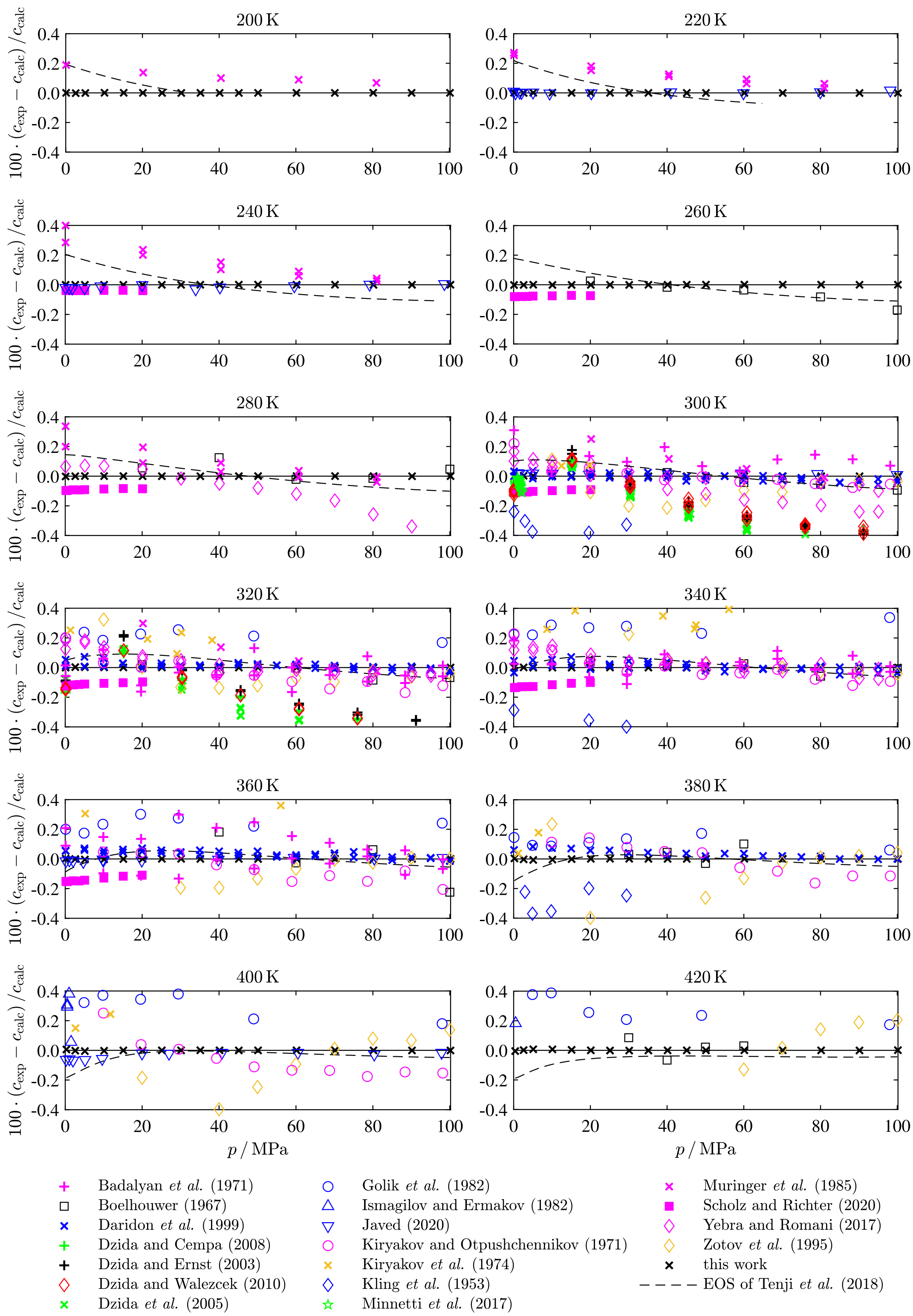

Fig. 9. Relative deviations of our experimental speeds of sound c_{exp} in n-heptane along the twelve measured isotherms, data of other authors from the literature [11–22,24,27,28,30,31,51] at nearby temperatures within ±10 K of the isotherms, and the equation of state of Tenji et al. [67] implemented in REFPROP [41] from values c_{calc} calculated with our speed-of-sound correlation, Eq. 5, as a function of pressure p.

Table 7
Details of selected literature data sets for the speed of sound in liquid isooctane.[a]

Authors	Year	Method	f/MHz	Purity/%	Data points	T/K	p/MPa	$U(c)$/%
Liquid at atmospheric pressure								
Freyer et al. [52]	1929	IF	0.414	n.r.	2	293 and 318	0.1	0.01
Subrahmanyam and Rajagopal [77]	1973	IF	3	n.r.	3	298–323	0.1	0.01
Rajagopal and Subrahmanyam [76]	1974	IF	3	n.r.	3	298–323	0.1	0.01
Aminabhavi et al. [43]	1994	IF	1	99.7	5	298–318	0.1	0.17
Takigawa and Tamura [78]	2000	SA	2	n.r.	2	298	0.1	n.r.
Ali et al. [68]	2006	IF	3	99.0	2	308	0.1	n.r.
Gómez-Días [71]	2006	DSA		99.0	5	293–323	0.1	0.007
Gonzales-Olmos and Iglesias [73]	2007	DSA		99.5	3	288–323	0.1	0.11
Gonzales-Olmos et al. [72]	2007	DSA		99.5	15	288–323	0.1	0.11
Morávková et al. [74]	2009	DSA		99.5	4	298–328	0.1	0.1
Fortin et al. [70]	2013	DSA		SRM 2214	14	278–343	0.083	0.05
Morávková et al. [75]	2013	DSA		99.5	4	298–328	0.1	0.1
Luning Prak et al. [56]	2014	DSA		99.6	11	293–343	0.1	0.06
Saturated liquid								
Awwad and Pethrick [69]	1983	SFAR	2	99.5	17	233–313	0.1	0.1
Liquid at elevated pressures								
Plantier and Daridon [32]	2005	PE	3	99.0	144	293–373	0.1–150	0.12
Zhang et al. [33]	2018	LS		99.8	215	294–632	0.1–12	1.3
This work	2025	PE	8	99.8	192	200–420	0.1–100	0.015

[a] Abbreviations: DSA: densimeter and sound analyzer (Anton Paar DSA 5000 M), IF: interferometer, n.r.: not reported, LS: light scattering, PE: pulse-echo method, SA: sing-around technique, SFAR: swept frequency acoustic resonator, and SRM 2214: NIST standard reference material 2214.

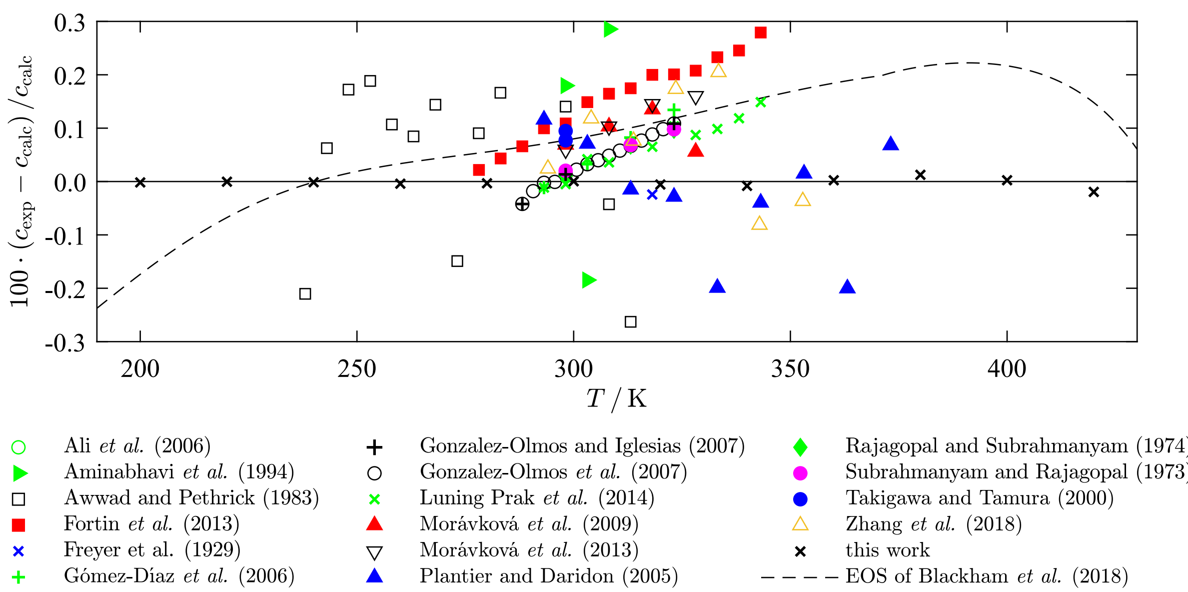

Fig. 10. Relative deviations of our experimental speeds of sound c_{exp} in isooctane at ambient pressure, data of other authors from the literature [32,33,43,52,56,68–78], and the equation of state of Blackham et al. [79] implemented in REFPROP [41] from values c_{calc} calculated with our speed-of-sound correlation, Eq. 5, as a function of temperature T. Above the normal boiling point of isooctane, deviations of our data slightly above the vapor pressure are shown.

commercial benchtop speed-of-sound instruments, exhibit a different temperature dependence than our data. This difference is probably due to the fact that the benchtop instruments were only calibrated at a single temperature near ambient, while the acoustic path length in our speed of sound sensor was calibrated in the whole measured temperature range. We recommend to calibrate the speed-of-sound sensor of such benchtop instruments also in the whole temperature range of the measurements with liquid water, for which the speed of sound is very accurately known. When such a calibration procedure is applied, it should be possible to measure the temperature dependence of the speed of sound more accurately.

CRediT authorship contribution statement

T. Dietl: Writing – original draft, Visualization, Validation, Software, Methodology, Investigation, Formal analysis, Data curation. **A. El Hawary:** Writing – original draft, Visualization, Validation, Software, Methodology, Investigation, Formal analysis, Data curation. **K. Meier:** Writing – review & editing, Writing – original draft, Visualization, Validation, Supervision, Resources, Project administration, Methodology, Investigation, Formal analysis, Conceptualization.

Declaration of competing interest

The authors declare that they have no known competing financial interests or personal relationships that could have appeared to influence the work reported in this paper.

Data availability

The data that support the findings of this study are available within this article.

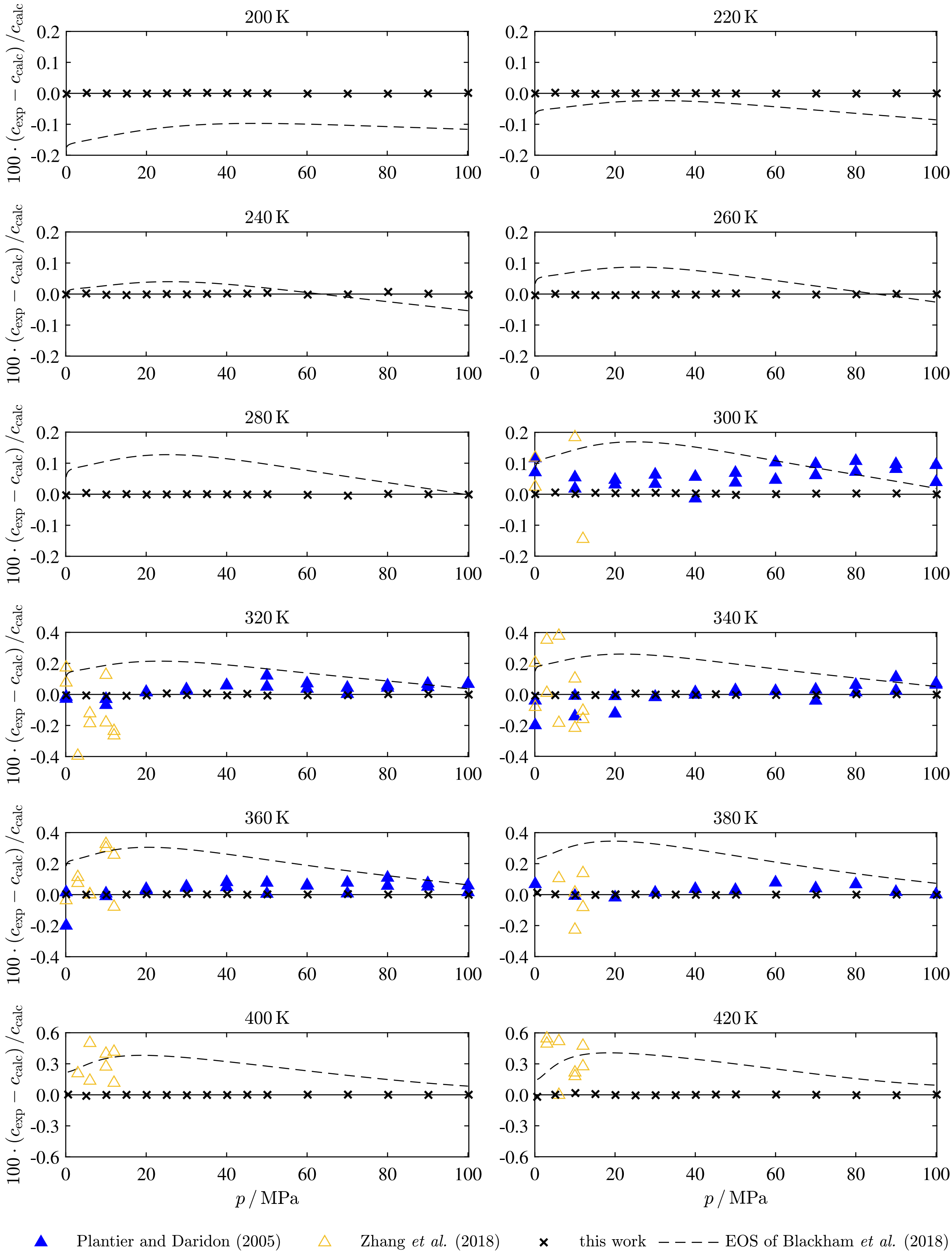

Fig. 11. Relative deviations of our experimental speeds of sound c_{exp} in isooctane at elevated pressures along isotherms, the data of Plantier and Daridon [32] and Zhang et al. [33] at nearby temperatures within ±10 K of the isotherms, and the equation of state of Blackham et al. [79] implemented in REFPROP [41] from values c_{calc} calculated with our speed-of-sound correlation, Eq. 5, as a function of pressure p.

References

[1] A. El Hawary, K. Meier, Measurements of the speed of sound in liquid and supercritical ethane, Fluid Phase Equilibr. 418 (2016) 125–132, http://dx.doi.org/10.1016/j.fluid.2015.11.019.

[2] K. Meier, S. Kabelac, Thermodynamic properties of propane. IV. Speed of sound in the liquid and supercritical regions, J. Chem. Eng. Data 57 (2012) 3391–3398, http://dx.doi.org/10.1021/je300466a.

[3] A. El Hawary, K. Meier, Measurements of the speed of sound in liquid *n*-butane, J. Chem. Eng. Data 61 (2016) 3858–3867, http://dx.doi.org/10.1021/acs.jced.6b00577.

[4] A. El Hawary, K. Meier, Speed-of-sound measurements and derived thermodynamic properties of liquid isobutane, J. Chem. Eng. Data 63 (2018) 3684–3703, http://dx.doi.org/10.1021/acs.jced.8b00202.

[5] A. El Hawary, S.Z. Mirzaev, K. Meier, Speed-of-sound measurements in liquid *n*-pentane and isopentane, J. Chem. Eng. Data 65 (2020) 1243–1263, http://dx.doi.org/10.1021/acs.jced.9b00602.

[6] G. Edgar, Measurement of knock characteristics of gasoline in terms of a standard fuel, Ind. Eng. Chem. 19 (1927) 145–146, http://dx.doi.org/10.1021/ie50205a049.

[7] B. Elvers, A. Schütze, Handbook of Fuels: Energy Sources for Transportation, Wiley-VCH, Weinheim, Germany, 2021.

[8] R. Span, Multiparameter Equations of State, Springer, Berlin, 2000.

[9] E.W. Lemmon, M.O. McLinden, W. Wagner, Thermodynamic properties of propane. III. A reference equation of state for temperatures from the melting line to 650 K and pressures up to 1000 MPa, J. Chem. Eng. Data 54 (2009) 3141–3180, http://dx.doi.org/10.1021/je900217v.

[10] J.P.M. Trusler, Physical Acoustics and Metrology of Fluids, Adam Hilger, Bristol, 1991.

[11] R. Kling, E. Nicolini, J. Tissot, Application of ultrasonics in the study of the elastic properties of hydrocarbons over a wide range of temperature and pressure, Rech. Aeronaut. 31 (1953) 31–36.

[12] J.W.M. Boelhouwer, Sound velocities in and adiabatic compressibilities of liquid alkanes at various temperatures and pressures, Physica 34 (1967) 484–492, http://dx.doi.org/10.1016/0031-8914(67)90016-X.

[13] A.L. Badalyan, N.F. Otpushchennikov, Y.S. Shoitov, Speed of sound in *n*-hexane, *n*-heptane and *n*-nonane as a function of pressure and temperature, Uc. Zap.- Kursk. Gos. Ped. Inst. 91 (1971) 135–143.

[14] B.S. Kiryakov, N.F. Otpushchennikov, About the dependence of the speed of sound in liquids on pressure, Uc. Zap.- Kursk. Gos. Ped. Inst. 91 (1971) 104–112.

[15] B.S. Kiryakov, N.F. Otpushchennikov, P.P. Panin, On the methodology of the calculation of the thermodynamic properties of *n*-alkanes from ultrasonic measurements with pressures up to 1000 atm, VINITI 800–74DEP (1974) 1–14.

[16] A.Z. Golik, I.I. Adamenko, M.G. Makhno, Complex apparatus for studying the density and velocity of ultrasound in liquids in a wide range of temperatures and pressures, Fiz. Zhidk. Sostoyaniya 10 (1982) 3–7.

[17] R.G. Ismagilov, G.V. Ermakov, Speed of sound in some superheated organic liquids, Teplofiz. Vys. Temp. 20 (1982) 677–682.

[18] M.J.P. Muringer, N.J. Trappeniers, S.N. Biswas, The effect of pressure on the sound velocity and density of toluene and *n*-heptane up to 2600 bar, Phys. Chem. Liq. 14 (1985) 273–296, http://dx.doi.org/10.1080/00319108508080991.

[19] V.V. Zotov, Y.F. Melikhov, G.A. Melnikov, Y.A. Neruchev, Sound Velocity in Liquid Hydrocarbons, Kursk State Pedagogical University, Kursk, Russia, 1995.

[20] J.L. Daridon, B. Lagourette, A. Lagrabette, Acoustic determination of thermodynamic properties of ternary liquid mixtures up to 150 MPa, Phys. Chem. Liq. 37 (1999) 137–160, http://dx.doi.org/10.1080/00319109908045122.

[21] M. Dzida, S. Ernst, Speed of sound in propan-1-ol + heptane mixtures under elevated pressures, J. Chem. Eng. Data 48 (2003) 1453–1457, http://dx.doi.org/10.1021/je030136n.

[22] M. Dzida, A. Żak, S. Ernst, Thermodynamic and acoustic properties of binary mixtures of alcohols and alkanes. I. Speed of sound in (ethanol+*n*-heptane) under elevated pressures, J. Chem. Thermodyn. 37 (2005) 405–414, http://dx.doi.org/10.1016/j.jct.2004.10.001.

[23] M. Dzida, P. Góralski, Excess molar heat capacities for (decan-1-ol+*n*-heptane) at temperatures from (290 to 318) K. Experimental results and theoretical description using the ERAS model, J. Chem. Thermodyn. 38 (2006) 962–969, http://dx.doi.org/10.1016/j.jct.2005.10.009.

[24] M. Dzida, M. Cempa, Thermodynamic and acoustic properties of (heptane+dodecane) mixtures under elevated pressures, J. Chem. Thermodyn. 40 (2008) 1531–1541, http://dx.doi.org/10.1016/j.jct.2008.05.014.

[25] V.H. Hasanov, The speed of sound of *n*-heptane, *n*-octane and their binary mixtures at temperatures T=293.15 to 523.15 K and pressures up to 60 MPa, High Temp. 50 (2012) 44–51, http://dx.doi.org/10.1134/S0018151X12010063.

[26] X. Zheng, Y. Zhang, M. He, Measurement of the speed of sound in hexane and heptane at temperatures from (303.15 to 536.15) K and pressures from (1.0 to 8.5) MPa, J. Chem. Eng. Data 61 (2016) 701–711, http://dx.doi.org/10.1021/je501106d.

[27] E. Minnetti, G. Pandarese, P. Evangelisti, F.R. Verdugo, C. Ungaro, A. Bastari, N. Paone, Dynamic measurement of speed of sound in *n*-heptane by ultrasonics during fuel injections, Ultrasonics 81 (2017) 39–49, http://dx.doi.org/10.1016/j.ultras.2017.05.012.

[28] F. Yebra, J. Troncoso, L. Romaní, Fully automatized apparatus for determining speed of sound for liquids in the temperature and pressure interval (283.15–343.15) K and (0.1–95) MPa, J. Chem. Thermodyn. 104 (2017) 102–109, http://dx.doi.org/10.1016/j.jct.2016.09.022.

[29] Y. Zhang, Y. Chen, T. Zhan, M. He, Measurement of the speed of sound in near-critical and supercritical *n*-heptane at temperatures from (513.40 to 650.90) K and pressures from (2.5 to 10.0) MPa, J. Chem. Eng. Data 63 (2018) 3331–3337, http://dx.doi.org/10.1021/acs.jced.8b00212.

[30] M.A. Javed, Speed of Sound Measurement for Industrially Important Fluids with the Pulse-Echo Technique (Ph.D. thesis), TU Berlin, 2020, http://dx.doi.org/10.14279/DEPOSITONCE-10693.

[31] C.W. Scholz, M. Richter, Speeds of sound in *n*-hexane and *n*-heptane at temperatures from (233.33 to 353.21) K and pressures up to 20 MPa, Int. J. Thermophys. 42 (2021) 18, http://dx.doi.org/10.1007/s10765-020-02778-6.

[32] F. Plantier, J.L. Daridon, Speed of sound of 2-methylpentane, 2,3-dimethylpentane, and 2,2,4-trimethylpentane from (293.15 to 373.15) K and up to 150 MPa, J. Chem. Eng. Data 50 (2005) 2077–2081, http://dx.doi.org/10.1021/je0502849.

[33] Y. Zhang, Y. Chen, Y. Zheng, X. He, M. He, Measurements of the speed of sound in liquid and supercritical *n*-octane and isooctane, J. Chem. Eng. Data 63 (2018) 102–112, http://dx.doi.org/10.1021/acs.jced.7b00712.

[34] K. Meier, The pulse-echo method for high-precision measurements of the speed of sound in fluids (Postdoctoral Thesis), Fachbereich Maschinenbau, Helmut-Schmidt-Universität/Universität der Bundeswehr Hamburg, Hamburg, Germany, 2006.

[35] K. Meier, S. Kabelac, Speed of sound instrument for fluids with pressures up to 100 MPa, Rev. Sci. Instrum. 77 (2006) 123903, http://dx.doi.org/10.1063/1.2400019.

[36] A.F. Estrada-Alexanders, J.P.M. Trusler, The speed of sound in gaseous argon at temperatures between 110 K and 450 K and at pressures up to 19 MPa, J. Chem. Thermodyn. 27 (1995) 1075–1089, http://dx.doi.org/10.1006/jcht.1995.0113.

[37] J.C. Brice, Crystals for quartz resonators, Rev. Modern Phys. 57 (1985) 105–146, http://dx.doi.org/10.1103/RevModPhys.57.105.

[38] FEZEN Datenbank für Stähle und NE-Metalle, Blatt 1.4571.41.03.0, Physikalische Eigenschaften nach SEW 310, Tafel 43, DVS Verlag, Düsseldorf, Germany, 2000.

[39] O. Kunz, W. Wagner, The GERG-2008 wide-range equation of state for natural gases and other mixtures: An expansion of GERG-2004, J. Chem. Eng. Data 57 (2012) 3032–3091, http://dx.doi.org/10.1021/je300655b.

[40] I.H. Bell, E.W. Lemmon, Automatic fitting of binary interaction parameters for multi-fluid Helmholtz-energy-explicit mixture models, J. Chem. Eng. Data 61 (2016) 3752–3760, http://dx.doi.org/10.1021/acs.jced.6b00257.

[41] E.W. Lemmon, I.H. Bell, M.L. Huber, M.O. McLinden, NIST Reference Fluid Thermodynamic and Transport Properties Database (REFPROP, version 10.0); NIST Standard Reference Database 23, in: Standard Reference Data Program, National Institute of Standards and Technology, Gaithersburg, MD, 2018.

[42] E. Alonso, H. Guerrero, D. Montaño, C. Lafuente, H. Artigas, Thermophysical study of the *n*-hexane or *n*-heptane with 1-chloropropane systems, Thermochim. Acta 525 (2011) 71–77, http://dx.doi.org/10.1016/j.tca.2011.07.023.

[43] T.M. Aminabhavi, M.I. Aralaguppi, B. Gopalakrishna, R.S. Khinnavar, Densities, shear viscosities, refractive indices, and speeds of sound of bis(2-methoxyethyl) ether with hexane, heptane, octane, and 2,2,4-trimethylpentane in the temperature interval 298.15-318.15 K, J. Chem. Eng. Data 39 (1994) 522–528, http://dx.doi.org/10.1021/je00015a028.

[44] M. Basu, T. Samanta, D. Das, Volumetric and acoustic properties of binary mixtures of tri-*n*-butyl phosphate with *n*-hexane, cyclohexane, and *n*-heptane from T=(298.15 to 323.15) K, J. Chem. Thermodyn. 57 (2013) 335–343, http://dx.doi.org/10.1016/j.jct.2012.09.015.

[45] A. Blanco, A. Gayol, D. Gómez, J.M. Navaza, Temperature dependence of thermophysical properties of ethanol + *n*-hexane + *n*-heptane, Phys. Chem. Liq. 51 (2013) 381–403, http://dx.doi.org/10.1080/00319104.2012.753601.

[46] C.A. Cerdeiriña, C.A. Tovar, D. González-Salgado, E. Carballo, L. Romaní, Isobaric thermal expansivity and thermophysical characterization of liquids and liquid mixtures, Phys. Chem. Chem. Phys. 3 (2001) 5230–5236, http://dx.doi.org/10.1039/B104891K.

[47] P.F. Cholpan, V.S. Sperkach, L.N. Garkusha, Study of physical properties of solutions of liquid paraffins along the equilibrium curve, Fiz. Zhidk. Sostoyaniya 9 (1983) 79–84.

[48] M. Chorążewski, M. Tkaczyk, Heat capacity, speed of ultrasound, and density for 1,5-dibromopentane + heptane within the temperature range from 293.15 K to 313.15 K, J. Chem. Eng. Data 51 (2006) 1825–1831, http://dx.doi.org/10.1021/je060200b.

[49] M. Chorążewski, P. Góralski, M. Hrynko, J.-P. Grolier, E. Wilhelm, Thermodynamic and acoustic properties of mixtures of 1,6-dichlorohexane with heptane from (293 to 313) K, J. Chem. Eng. Data 55 (2010) 5471–5477, http://dx.doi.org/10.1021/je100610v.

[50] R. Devi, S. Gahlyan, M. Rani, S. Maken, Thermodynamic and acoustic properties of binary mixtures of diisopropyl ether, benzene and alkanes at 298.15, 308.15 and 318.15 K: Prigogine-Flory-Patterson theory and graph theory, J. Mol. Liq. 275 (2019) 364–377, http://dx.doi.org/10.1016/j.molliq.2018.11.045.

[51] M. Dzida, L. Waleczek, Speed of sound, density, and heat capacity for (2-methyl-2-butanol+heptane) at pressures up to 100 MPa and temperatures from (293 to 318) K. Experimental results and theoretical investigations, J. Chem. Thermodyn. 42 (2010) 312–322, http://dx.doi.org/10.1016/j.jct.2009.09.001.

[52] E.B. Freyer, J.C. Hubbard, D.H. Andrews, Sonic studies of the physical properties of liquids I. The sonic interformeter. The velocity of sound in some organic liquids and their compressibilities, J. Am. Chem. Soc. 51 (1929) 759–770, http://dx.doi.org/10.1021/ja01378a014.

[53] A.Z. Golik, P.F. Cholpan, Investigation of the velocity of ultrasound in some polysiloxanes, Akust. Zh. 7 (1961) 33–39.

[54] A.Z. Golik, I.I. Ivanova, Molekular structure, density, compressibility, and shear viscosity of *n*-paraffins in liquid phase, Zh. Fiz. Khim. 36 (1962) 1768–1770.

[55] B.N. Kireev, N.F. Otpushchennikov, Velocity of sound in certain *n*-alkanes along the saturation line at low temperatures, Russ. J. Phys. Chem. 48 (1974) 829–831.

[56] D.J. Luning Prak, J.S. Cowart, P.C. Trulove, Density, viscosity, speed of sound, bulk modulus, and surface tension of binary mixtures of *n*-heptane + 2,2,4-trimethylpentane at (293.15 to 338.15) K and 0.1 MPa, J. Chem. Eng. Data 59 (2014) 3842–3851, http://dx.doi.org/10.1021/je5007532.

[57] G. Marino, M.M. Piñeiro, M. Iglesias, B. Orge, J. Tojo, Temperature dependence of binary mixing properties for acetone, methanol, and linear aliphatic alkanes (C_6–C_8), J. Chem. Eng. Data 46 (2001) 728–734, http://dx.doi.org/10.1021/je000200q.

[58] L. Martínez-Baños, C. Rivas, J.M. Embid, S. Otín, Excess molar volumes and speed of sound in bromotrichloromethane + *n*-heptane, dibromomethane + *n*-heptane, bromotrichloromethane + dibromomethane, and bromotrichloromethane + bromochloromethane at temperatures from (293.15 to 313.15) K, J. Chem. Eng. Data 58 (2013) 248–256, http://dx.doi.org/10.1021/je300775u.

[59] G.A. Melnikov, V.N. Verveiko, N.F. Otpushchennikov, Complex study of the elastic and thermal properties of hydrocarbons and their halogen derivatives by the acoustic method, Russ. J. Phys. Chem. 62 (1988) 393–394.

[60] K. Moodley, Density, speed of sound, and refractive index measurements for mixtures of *n*-heptane with pentan-2-one or 4-methylpentan-2-one for T=298.15–338.15 K and 0.101 MPa, J. Chem. Eng. Data 65 (2020) 1761–1772, http://dx.doi.org/10.1021/acs.jced.9b01070.

[61] Y.A. Neruchev, V.V. Zotov, N.F. Otpushchennikov, Velocity of sound in the homologous series of *n*-alkanes, Russ. J. Phys. Chem. 43 (1969) 1597–1599.

[62] Y.A. Neruchev, M.F. Bolotnikov, V.V. Zotov, Investigation of ultrasonic velocity in organic liquids on the saturation curve, High Temp. 43 (2005) 266–309, http://dx.doi.org/10.1007/s10740-005-0067-7.

[63] A. Przybyła, M. Chorążewski, E. Zorębski, W. Marczak, Thermodynamic and acoustic properties of mixtures of dibromomethane + heptane, Int. J. Thermophys. 32 (2011) 852–866, http://dx.doi.org/10.1007/s10765-010-0773-1.

[64] V.S. Sperkach, P.F. Cholpan, V.N. Sinilo, A.V. Zolotar, Spread of ultrasonic waves in isoviscous solutions of *n*-paraffins, Fiz. Zhidk. Sostoyaniya 7 (1979) 110–113.

[65] V.V. Zotov, Y.A. Neruchev, N.F. Otpushchennikov, Some thermodynamic properties of *n*-heptane on the saturation line, J. Eng. Phys. 15 (1968) 1098–1099.

[66] V.V. Zotov, B.N. Kireev, Y.A. Neruchev, Study of the equilibrium properties of hydrocarbons on the saturation line by an accoustic method, J. Appl. Mech. Technol. Phys. 16 (1975) 282–284.

[67] D. Tenji, M. Thol, E.W. Lemmon, R. Span, Helmholtz equation of state for *n*-heptane (unpublished results).

[68] A. Ali, A.K. Nain, D. Chand, R. Ahmad, Volumetric, ultrasonic, viscometric and refractive index behavior of binary mixtures of 2,2,4-trimethylpentane with aromatic hydrocarbons: An experimental and theoretical study, J. Mol. Liq. 128 (2006) 32–41, http://dx.doi.org/10.1016/j.molliq.2005.02.007.

[69] A.M. Awwad, R.A. Pethrick, Adiabatic compressibility of branched chain hydrocarbons- pentanes and hexanes, J. Mol. Liq. 25 (1983) 115–127, http://dx.doi.org/10.1016/0167-7322(83)80014-2.

[70] T.J. Fortin, A. Laesecke, M. Freund, S. Outcalt, Advanced calibration, adjustment, and operation of a density and sound speed analyzer, J. Chem. Thermodyn. 57 (2013) 276–285, http://dx.doi.org/10.1016/j.jct.2012.09.009.

[71] D. Gómez-Díaz, J.C. Mejuto, J.M. Navaza, Density, viscosity, and speed of sound of solutions of AOT reverse micelles in 2,2,4-trimethylpentane, J. Chem. Eng. Data 51 (2006) 409–411, http://dx.doi.org/10.1021/je050333h.

[72] R. Gonzalez-Olmos, M. Iglesias, Temperature influence on mixing properties of {ethyl tert-butyl ether (ETBE)+gasoline additives}, J. Chem. Thermodyn. 39 (2007) 1557–1564, http://dx.doi.org/10.1016/j.jct.2007.05.005.

[73] R. Gonzalez-Olmos, M. Iglesias, J.M. Goenaga, J.M. Resa, Influence of temperature on thermodynamic properties of methyl t-butyl ether (MTBE) + gasoline additives, Int. J. Thermophys. 28 (2007) 1199–1227, http://dx.doi.org/10.1007/s10765-007-0223-x.

[74] L. Morávková, Z. Wagner, J. Linek, Volumetric behaviour of binary liquid systems composed of toluene, isooctane, and methyl tert-butyl ether at temperatures from (298.15 to 328.15) K, J. Chem. Thermodyn. 41 (2009) 591–597, http://dx.doi.org/10.1016/j.jct.2009.01.008.

[75] L. Morávková, J. Troncoso, K. Machanová, Z. Sedláková, Volumetric behaviour of the (2,2,4-trimethylpentane + methylbenzene + butan-1-ol) ternary system and its binary subsystems within the temperature range (298.15–328.15) K, J. Chem. Thermodyn. 64 (2013) 137–150, http://dx.doi.org/10.1016/j.jct.2013.05.009.

[76] E. Rajagopal, S.V. Subrahmanyam, Excess functions V^{E}, $(\partial V^{\mathrm{E}}/\partial p)_T$, and C_p^{E} of isooctane + benzene and + toluene, J. Chem. Thermodyn. 6 (1974) 873–876, http://dx.doi.org/10.1016/0021-9614(74)90231-6.

[77] S.V. Subrahmanyam, E. Rajagopal, Excess thermodynamic functions of the systems isooctane + carbon tetrachloride and isooctane + cyclohexane, Z. Phys. Chem. 85 (1973) 256–268, http://dx.doi.org/10.1524/zpch.1973.85.5_6.256.

[78] T. Takigawa, K. Tamura, Thermodynamic properties of (1,3-dioxane, or 1,4-dioxane + a non-polar liquid) at $T = 298.15$ K; speed of sound, excess isentropic and isothermal compressibilities and excess isochoric heat capacity, J. Chem. Thermodyn. 32 (2000) 1045–1055, http://dx.doi.org/10.1006/jcht.2000.0676.

[79] T.M. Blackham, A.K. Lemmon, E.W. Lemmon, Helmholtz equation of state for isooctane (unpublished results).

[80] W. Wagner, A mathematical-statistical method for establishing thermodynamic equations – demonstrated using the vapor pressure curve of pure fluid substances as an example. Fortschr.-Ber. VDI-Z. Reihe 3, Nr. 39, 1974.

[81] A. El Hawary, K. Meier, Thermodynamic properties of liquid toluene and *n*-butane determined from speed of sound data, Int. J. Thermophys. 43 (2022) 71, http://dx.doi.org/10.1007/s10765-021-02958-y.

[82] A.H. Harvey, What the thermophysical property community should know about temperature scales, Int. J. Thermophys. 42 (2021) 165, http://dx.doi.org/10.1007/s10765-021-02915-9.

[83] V. Diky, C.D. Muzny, A.F. Kazakov, E. Paulechka, E.W. Lemmon, A. Bazyleva, S.A. Townsend, T. Renken, A.Y. Smolyanitsky, R.D. Chirico, M. Frenkel, J.W. Magee, K.G. Kroenlein, ThermoData Engine (TDE Version 10.4.5.a): Pure compounds, NIST Standard Reference Database 103a, Standard Reference Data Program; National Institute of Standards and Technology, Gaithersburg, MD, 2023.

[84] DDBST Dortmund Data Bank Software & Separation Technology GmbH, Dortmund Data Bank 2022, 2022, Oldenburg, Germany.

[85] J. Canosa, A. Rodríguez, J. Tojo, Binary mixture properties of diethyl ether with alcohols and alkanes from 288.15 K to 298.15 K, Fluid Phase Equilibr. 156 (1999) 57–71, http://dx.doi.org/10.1016/S0378-3812(99)00032-1.

[86] A. Gayol, M. Iglesias, J.M. Goenaga, R.G. Concha, J.M. Resa, Temperature influence on solution properties of ethanol + *n*-alkane mixtures, J. Mol. Liq. 135 (2007) 105–114, http://dx.doi.org/10.1016/j.molliq.2006.11.012.

[87] K. Meier, S. Kabelac, Measurements of the speed of sound in liquid toluene, J. Chem. Eng. Data 58 (2013) 1398–1406, http://dx.doi.org/10.1021/je4001697.